

Particle production in field theories coupled to strong external sources

I. Formalism and main results

François Gelis⁽¹⁾, Raju Venugopalan⁽²⁾

September 18, 2018

1. Service de Physique Théorique, URA 2306 du CNRS
CEA/DSM/Saclay, Bât. 774
91191, Gif-sur-Yvette Cedex, France
2. Department of Physics, Bldg. 510 A,
Brookhaven National Laboratory,
Upton, NY-11973, USA

Abstract

We develop a formalism for particle production in a field theory coupled to a strong time-dependent external source. An example of such a theory is the Color Glass Condensate. We derive a formula, in terms of cut vacuum-vacuum Feynman graphs, for the probability of producing a given number of particles. This formula is valid to all orders in the coupling constant. The distribution of multiplicities is non-Poissonian, even in the classical approximation. We investigate an alternative method of calculating the mean multiplicity. At leading order, the average multiplicity can be expressed in terms of retarded solutions of classical equations of motion. We demonstrate that the average multiplicity at *next-to-leading order* can be formulated as an initial value problem by solving equations of motion for small fluctuation fields with retarded boundary conditions. The variance of the distribution can be calculated in a similar fashion. Our formalism therefore provides a framework to compute from first principles particle production in proton-nucleus and nucleus-nucleus collisions beyond leading order in the coupling constant and to all orders in the source density. We also provide a transparent interpretation (in conventional field theory language) of the well known Abramovsky–Gribov–Kancheli (AGK) cancellations. Explicit connections are made between the framework for multi-particle production developed here and the framework of Reggeon field theory.

Preprint SPhT-T06/009

1 Introduction

The study of multiparticle production in hadron collisions at high energies is an outstanding problem in the study of the strong interactions. With the advent of QCD, it was understood that semi-hard particle production in high energy hadronic interactions is dominated by interactions between partons having a small fraction x of the longitudinal momentum of the incoming nucleons. In the Regge limit of small x and fixed momentum transfer squared Q^2 – corresponding to very large center of mass energies squared s – the Balitsky-Fadin-Kuraev-Lipatov (BFKL) evolution equation [1,2] predicts that parton densities grow very rapidly with decreasing x . Because this rapid growth in the Regge limit corresponds to very large phase space densities of partons in hadronic wavefunctions, it was proposed that saturation effects may play an important role in hadronic collisions at very high energies [3,4,5,6]. Saturation effects slow down the growth of parton densities relative to that of BFKL evolution and may provide the mechanism for the unitarization of cross-sections at high energies.

The large phase space density suggests that the small x partons can be described by a classical color field rather than as particles [7,8,9]. More precisely, the McLerran-Venugopalan (MV) model proposes a dual description, whereby small x partons are described by a classical field and the large x partons act as color sources for the classical field. The original model considered a large nucleus containing a large number of large x partons (at least $3A$ valence quarks where A is the atomic number of the nucleus). In this limit, they produce a strong color source and one has to solve the full classical Yang-Mills equations to find the classical field. This procedure properly incorporates the recombination interactions that are responsible for gluon saturation. In the MV model, the large x color sources are described by a Gaussian statistical distribution [7,10]. A more general form of this statistical distribution, for $SU(N_c)$ gauge theories, valid for large A and moderate x , is given in Ref. [11,12].

The separation between large x and small x , inherent to the dual description of the MV model, is somewhat arbitrary and has been exploited to derive a renormalization group (RG) equation, the JIMWLK equation [13,14,15,16,17,18,19,20]. This functional RG equation describes the change in the statistical distribution of color sources with x . It can be expressed as an infinite hierarchy of evolution equations for correlators [21], and has a useful (and tremendously simpler) large N_c and large A mean-field approximation [22], known as the Balitsky-Kovchegov equation. This general framework is often referred to as the Color Glass Condensate (CGC) [23,24,25].

The discussion above refers to the properties of hadronic wave functions at high energies. To compute particle production in the CGC framework, (a) one must find the distribution of color sources in the projectiles, either by solving the JIMWLK equation or by using a model such as the MV model, and (b) one must calculate the production of the relevant particles from the sources. In this paper, we will assume that the source distributions are known and shall focus on particle production in the presence of these sources.

At leading order, one knows how to compute the production of quarks and

gluons from strong color sources. Inclusive gluon production is obtained by solving the classical Yang-Mills equations for two color sources moving at the speed of light in opposite directions [26,27,28]. This problem has been solved numerically in [29,30,31,32,33,34] for the boost-invariant case. A first computation for the boost non-invariant case has also been performed recently [35]. The multiplicity of quark-pairs is computed from the quark propagator in the background field of [29,30,31,32,33,34] – it has been studied numerically in [36,37].

These results summarize the state of the art in studies of particle production from strong classical color sources. In the present paper, we will systematically examine particle production in a field theory coupled to an external time-dependent classical source. In particular, we will consider how one computes results beyond the above mentioned leading order results. To avoid the technical complications of gauge theories, we shall focus our discussion on the theory of a real scalar field. The complexities of QCD, such as gauge invariance, are of course extremely important. However, several of the lessons gained from the simpler theory considered here should also apply to studies of particle production in QCD. These will be applied in follow ups to this paper.

This paper is organized as follows. We begin, in the next section, by setting up the model. We recall well known results for counting powers of the coupling constant and of the powers of \hbar ; in particular we discuss how these are modified for field theories with strong external sources. We discuss the vacuum-vacuum diagrams that will play a crucial role in the rest of the paper. We show clearly that the sum of the vacuum-vacuum diagrams is not a trivial phase (as is the case for field theories in the vacuum) but gives a non-trivial contribution to the probability in theories where the field is coupled to a time-dependent source.

In section 3, we use Cutkosky’s cutting rules to derive a formula for the probability P_n of producing n particles, in terms of cut vacuum-vacuum diagrams. This formula, for theories with strong sources, is new and is valid to all orders in the coupling constant. While the formula at this stage is not useful for explicit computations, it shows unambiguously that the distribution of the multiplicities of produced particles is not Poissonian, even in the classical approximation. We also derive a compact formula for the generating function $F(x)$ of the probabilities P_n .

In section 4, we discuss in detail the calculation of the first moment of the distribution, namely, the average multiplicity $\langle n \rangle = \sum_n n P_n$. We obtain a formula which is valid to all orders for $\langle n \rangle$. We work it out explicitly at leading and next-to-leading order. It is well known that the leading order expression can be expressed in terms of classical fields that are computed by solving partial differential equations, with retarded boundary conditions, for the classical fields. What is remarkable and a major result of this work is the fact that one can similarly compute the multiplicity at NLO from the small fluctuation fields (in the presence of the classical background field) with simple initial conditions at $x_0 = -\infty$, i.e. in terms of partial differential equations with retarded boundary conditions. *This result makes next-to-leading order computations of the average multiplicity feasible even in theories with strong external sources. It has possibly*

very significant ramifications for heavy ion collisions.

The results in section 3 and 4 are related in section 5. The Abramovsky-Gribov-Kancheli cancellations [39], originally formulated in the context of reggeon field theory models, play an important role in relating the inclusive particle multiplicities in 4 to moments of the probability distributions in 3. In section 5, we provide a “dictionary” to map the original AGK discussion formulated in the language of cut reggeons into our language of cut vacuum-vacuum diagrams in field theories with external sources. The fact that the AGK cancellations require a Poissonian distribution of cut reggeons is seen to follow naturally if one identifies reggeons (cut and uncut) with connected vacuum-vacuum sub-diagrams. This identification further leads us to the conclusion that there are further cancellations that are not visible when the discussion takes place at the level of reggeons. These additional cancellations simplify the calculation of the multiplicity $\langle n \rangle$ as well as that of higher moments. We end this section by a general formula that gives the variance of the distribution of produced particles.

In the final section, we provide a summary of the new results derived in this paper and of their possible ramifications for QCD at high energies. The paper contains four appendices. In appendix A, we give a very brief reminder of the Schwinger-Keldysh formalism. In appendix B, we derive the solution of the Lippmann-Schwinger equation (70). In appendix C, we discuss a proof demonstrating that the only distributions of cut reggeons that lead to AGK cancellations are Poisson distributions. In appendix D, we discuss details of the cancellations giving rise to the identity in eq. (109).

2 General framework

In this section, we will set the groundwork for the discussion in subsequent sections. Much of the material here is textbook fare and can be found, for instance, in refs. [48,49]. However, there are subtleties that distinguish the discussion of field theories in the presence of external sources to discussions of field theories in vacuum. These are emphasized throughout, especially in section 2.3.

2.1 Model

The model, for all the discussions in this paper, will be the theory of a real scalar field ϕ , with ϕ^3 self-interactions and with the field coupled to an external source $j(x)$. This simple scalar theory captures many of the key features of multi-particle production in QCD, while avoiding the complications arising from keeping track of the internal color degrees of freedom and the necessity of choosing a gauge in the latter.

Without further ado, the Lagrangian density in our model is

$$\mathcal{L} \equiv \frac{1}{2} \partial_\mu \phi \partial^\mu \phi - \frac{1}{2} m^2 \phi^2 - \frac{g}{3!} \phi^3 + j \phi . \quad (1)$$

The reader should note that the coupling g in this theory is dimensionful, with dimensions of the mass; the theory therefore, in 4 dimensions, is super renormalizable. When we draw the Feynman diagrams for this theory, we will denote the source by a black dot. Keeping in mind applications of our results to the description of hadronic collisions in the Color Glass Condensate framework, one may think of $j(x)$ as the scalar analog of the sum of two source terms $j(x) = j_1(x) + j_2(x)$ corresponding respectively to the color currents of the two hadronic projectiles.

2.2 Power counting

Power counting is essential in understanding the perturbative expansion of amplitudes in this model. For theories with weak sources, where j is parametrically of order 1, the leading contributions would come from the diagrams with the least number of vertices. We are here interested in theories (such as the CGC) where the sources are strong. By strong, we mean specifically that the $j\phi$ term is of the same order as the other terms in the Lagrangian density. This implies that $gj(x)$ is of order unity, as opposed to $j(x) \sim 1$ itself. Therefore, as discussed further below, independent powers of g in any given diagram arise only if the vertex is not connected to a source. In this power counting scheme, the leading diagrams can have negative powers of g . We will subsequently also discuss the power counting in \hbar .

2.2.1 Powers of the coupling

For strong sources, $gj \sim 1$, attaching new sources to a given diagram does not change its order. There are therefore an infinity of diagrams contributing at a given order in g . For instance, even the classical approximation of this model, which involves only tree diagrams, resums an infinite number of contributions. Field theories coupled to a strong source are therefore non-trivial and exhibit rich properties *even if the coupling g is very small*.

To make this discussion more explicit, consider a generic simply connected diagram containing n_E external lines, n_I internal lines, n_L loops, n_J sources and n_V vertices. These parameters are not independent, but are related by the equations,

$$\begin{aligned} 3n_V + n_J &= n_E + 2n_I , \\ n_L &= n_I - n_V - n_J + 1 . \end{aligned} \tag{2}$$

Thanks to these two relations, the order of this diagram is

$$g^{n_V} j^{n_J} = g^{n_E + 2(n_L - 1)} (gj)^{n_J} . \tag{3}$$

As explained previously, when the source is as strong as $1/g$, the last factor is irrelevant; the order of the diagram depends only on its number of external legs and number of loops. Note also that the above formulas are only valid for a simply connected diagram: they must be applied independently to each

disconnected subdiagram of a more complicated diagram. Note in particular that a simply connected tree diagram ($n_L = 0$) with no external legs ($n_E = 0$) attached to strong sources is of order g^{-2} .

2.2.2 Powers of \hbar

It is also interesting to discuss the order in \hbar of a given diagram. Recall that \hbar has the dimension of an action. Therefore,

$$\frac{S}{\hbar} = \int d^4x \left[-\frac{1}{2}\phi \frac{G_0^{-1}}{\hbar} \phi - \frac{g}{3!\hbar} \phi^3 + \frac{j}{\hbar} \phi \right], \quad (4)$$

where G_0 is the free propagator. From this equation, it is clear that the following mnemonic can be applied to keeping track of powers of \hbar in the perturbative expansion:

- (i) a propagator brings a power of \hbar ,
- (ii) a vertex brings a power of $1/\hbar$,
- (iii) a source j brings a power of $1/\hbar$.

The order in \hbar of the generic diagram in the previous sub-section is therefore

$$\hbar^{n_E + n_I - n_V - n_J} = \hbar^{n_E + n_L - 1}. \quad (5)$$

We thus recover the well-known result that the order in \hbar , for a fixed number of external legs, depends only on the number of loops. For the purposes of this paper, it is important to note that the result does not depend on the number of insertions of the classical source in the diagram. Clearly this implies that arbitrarily complicated diagrams can be of the same order in \hbar . In the rest of this paper, we do not keep track of the powers of \hbar , and simply set $\hbar = 1$.

2.3 Vacuum–vacuum diagrams

The forthcoming discussion in the next section, of the multiplicity distributions of produced particles, will be formulated in terms of “vacuum–vacuum” diagrams in the presence of strong external sources. Vacuum–vacuum diagrams are simply Feynman diagrams without any external legs [48]. They contribute to the vacuum-to-vacuum transition amplitude $\langle 0_{\text{out}} | 0_{\text{in}} \rangle$ – hence the name. The perturbative expansion of any amplitude with external legs generates these vacuum–vacuum diagrams as disconnected factors.

When one considers a field theory in the vacuum (no external source: $j = 0$), one usually disregards vacuum–vacuum graphs because their sum is a pure phase that does not contribute to transition probabilities. That the sum of vacuum–vacuum diagrams, in this case, is a pure phase follows from the fact that no particles can be created if the initial state is the vacuum. The probability that the vacuum stays the vacuum is unity and the corresponding amplitude must be a pure phase.

The situation is very different in a theory, like the one under consideration, where the fields are coupled to an external source¹. Assume that this external source is such (time-dependent for instance) that an amplitude from the vacuum to a populated state is non-zero, namely,

$$\exists \beta \neq 0, \quad \langle \beta_{\text{out}} | 0_{\text{in}} \rangle \neq 0. \quad (6)$$

From unitarity,

$$\sum_{\beta} \left| \langle \beta_{\text{out}} | 0_{\text{in}} \rangle \right|^2 = 1, \quad (7)$$

we conclude that

$$\left| \langle 0_{\text{out}} | 0_{\text{in}} \rangle \right|^2 < 1. \quad (8)$$

Therefore, the amplitude $\langle 0_{\text{out}} | 0_{\text{in}} \rangle$ cannot be a pure phase.

It can be expressed as [48]

$$\langle 0_{\text{out}} | 0_{\text{in}} \rangle \equiv e^{i\mathcal{V}[j]}, \quad (9)$$

where $i\mathcal{V}[j]$ denotes² compactly the sum of the connected vacuum-vacuum diagrams in the presence of an external source j ,

$$i\mathcal{V}[j] \equiv i \sum_{\text{conn}} V = \frac{1}{2} \bullet\text{---}\bullet + \frac{1}{6} \bullet\text{---}\begin{array}{l} \bullet \\ \diagup \\ \bullet \end{array} + \frac{1}{8} \begin{array}{l} \bullet \\ \diagup \\ \bullet \end{array} \text{---} \begin{array}{l} \bullet \\ \diagdown \\ \bullet \end{array} + \frac{1}{8} \begin{array}{l} \bullet \\ \diagup \\ \bullet \end{array} \text{---} \begin{array}{l} \bullet \\ \diagdown \\ \bullet \end{array} + \dots \quad (10)$$

In the diagrammatic expansion on the right hand side, we have represented only tree diagrams, but of course $i\mathcal{V}[j]$ contains diagrams at any loop order. The number preceding each diagram is its symmetry factor. Note finally that because external lines are absent, the power counting of the previous subsection tells us that vacuum-vacuum diagrams come with powers that are given by

$$g^{2(n_L-1)}(gj)^{n_J}. \quad (11)$$

Therefore, in the presence of strong sources, $j \sim g^{-1}$, connected tree vacuum-vacuum diagrams are all of order g^{-2} , the 1-loop vacuum-vacuum diagrams are all of order 1, and so on.

It is the squared modulus of the vacuum–vacuum amplitude that contributes to the transition probability. This is simply $\exp(-2 \text{Im} \mathcal{V}[j])$. In the next section, we will discuss a method for computing $2 \text{Im} \mathcal{V}[j]$ directly.

¹For example, in the Color Glass Condensate (CGC) framework, incoming hadronic states are described by a pair of classical color sources to which the gauge fields couple. At high energies, such a separation is dictated by the kinematics. The resulting effective theory, the CGC, greatly simplifies the description of the initial state [6,23,24,25].

²The factor i is purely conventional here. It has been introduced for later convenience when we discuss cutting rules.

3 Multiplicity distribution from vacuum-vacuum diagrams

We will begin this section with a discussion of the cutting rules for vacuum-vacuum graphs in theories with external sources. These rules, for instance, can be employed to compute the imaginary part of the $\mathcal{V}[j]$ introduced in eq. (10). We will then present an intuitive discussion of how the probability for producing n -particles can be expressed in terms of cut vacuum-vacuum diagrams. We shall demonstrate the importance of the vacuum-vacuum factors in preserving unitarity for a theory with strong external sources. A generating function is introduced to compute moments of the distribution of probabilities; we will show that the distribution of probabilities is non-Poissonian, even for classical tree level graphs. In the final sub-section, we will present a formal expression of the intuitive arguments developed in the previous sub-sections.

3.1 Cutting rules

Let us first consider the analog of the Cutkosky rules [38] in our model. These will also prove useful for our discussion in the following section where we develop an alternative method to compute multiplicity distributions. One starts by decomposing the Feynman (time-ordered) free propagator in two pieces according to the time-ordering of the two endpoints³

$$G_F^0(x, y) \equiv \theta(x^0 - y^0)G_{-+}^0(x, y) + \theta(y^0 - x^0)G_{+-}^0(x, y). \quad (12)$$

This equation defines the propagators G_{-+}^0 and G_{+-}^0 . The notations for these objects have been chosen in analogy with the Schwinger-Keldysh formalism (see [50,51], and the brief summary in appendix A), for reasons that will become clear in section 4. Pursuing this analogy, the Feynman propagator G_F^0 is also denoted as G_{++}^0 . We introduce as well the (anti-time-ordered) propagator G_{--}^0 defined as

$$G_{--}^0(x, y) \equiv \theta(x^0 - y^0)G_{+-}^0(x, y) + \theta(y^0 - x^0)G_{-+}^0(x, y). \quad (13)$$

Note that the four propagators so defined are not independent; they are related by the identity,

$$G_{++}^0 + G_{--}^0 = G_{-+}^0 + G_{+-}^0. \quad (14)$$

In addition to these new propagators, we will consider two kinds of vertices, of type + or -. A vertex of type + is the ordinary vertex and appears with a factor $-ig$ in Feynman diagrams. A vertex of type - is the opposite of a + vertex, and its Feynman rule is $+ig$. Likewise, for insertions of the source j , insertions of type + appear with the factor $+ij(x)$ while insertions of type - appear instead with $-ij(x)$. The motivation for introducing these additional vertices and sources will become clearer shortly.

³The superscript 0 indicates **free** propagators.

For each Feynman diagram iV containing only “+” vertices and sources (denoted henceforth as $iV_{\{+\dots+\}}$) contributing to the sum of connected vacuum-vacuum diagrams, define a corresponding set of diagrams $iV_{\{\epsilon_i\}}$ by assigning the symbol ϵ_i to the vertex i of the original diagram (and connecting a vertex of type ϵ to a vertex of type ϵ' with the propagator $G_{\epsilon\epsilon'}^0$). Each ϵ_i can be either of the “+” or “-” type. The generalized set of diagrams includes 2^n such diagrams if the original diagram had n vertex and sources. These diagrams obey the so-called “largest time equation” [52,53]. If one examines these diagrams before the times at the vertices and sources have been integrated out, and assumes that the vertex or source with the largest time is numbered i , it is easy to prove that

$$iV_{\{\dots\epsilon_i\dots\}} + iV_{\{\dots-\epsilon_i\dots\}} = 0, \quad (15)$$

where the dots denote the exact same configuration of ϵ 's in both terms, for the vertices and sources that do not carry the largest time. This equation generalizes immediately to the constraint,

$$\sum_{\{\epsilon_i\}} iV_{\{\epsilon_i\}} = 0, \quad (16)$$

where the sum is extended to the 2^n possible configurations of the ϵ 's in the Feynman diagram of interest ⁴.

This well known identity, being true for arbitrary times and positions of the vertices and sources, is also valid for the Fourier transforms of the corresponding diagrams. To see this, we first write down the explicit expressions for the Fourier transforms of the propagators $G_{\pm\pm}^0$

$$\begin{aligned} G_{++}^0(p) &= \frac{i}{p^2 - m^2 + i\epsilon}, & G_{--}^0(p) &= \frac{-i}{p^2 - m^2 - i\epsilon}, \\ G_{-+}^0(p) &= 2\pi\theta(p^0)\delta(p^2 - m^2), & G_{+-}^0(p) &= 2\pi\theta(-p^0)\delta(p^2 - m^2). \end{aligned} \quad (17)$$

$G_{--}^0(p)$ is the complex conjugate of $G_{++}^0(p)$. Using these relations, one can show that

$$iV_{\{+\dots+\}} + iV_{\{-\dots-\}} = iV_{\{+\dots+\}} + (iV_{\{+\dots+\}})^* = -2\text{Im} V. \quad (18)$$

We can therefore rewrite the imaginary part of the original Feynman diagram V as

$$2\text{Im} V = \sum_{\{\epsilon_i\}'} iV_{\{\epsilon_i\}}, \quad (19)$$

where the prime in the sum indicates that the two terms where all the vertices and sources are of type + or all of type - are excluded from the sum.

For a given term in the right hand side of the above formula, one can divide the diagram in several disconnected subgraphs, each containing only + or only - vertices and sources⁵. The + regions and - regions of the diagram are

⁴For a recent application of largest time relations to QCD, we refer the reader to Ref. [54].

⁵Note that such disconnected subgraphs can exist only if they contain at least one external source. They would otherwise be forbidden by energy conservation.

separated by a “cut” – each diagram in the r.h.s. of eq. (19) is therefore a “cut vacuum-vacuum diagram”. At tree level, the first terms generated by these cutting rules (applied to compute the imaginary part of the sum of connected vacuum-vacuum diagrams) are

$$\begin{aligned}
2 \operatorname{Im} \mathcal{V}[j] = & \frac{1}{2} \cdot \text{diagram}_1 + \frac{1}{2} \cdot \text{diagram}_2 \\
& + \frac{1}{6} \cdot \text{diagram}_3 + \frac{1}{6} \cdot \text{diagram}_4 + \frac{1}{6} \cdot \text{diagram}_5 + \frac{1}{6} \cdot \text{diagram}_6 + \frac{1}{6} \cdot \text{diagram}_7 + \frac{1}{6} \cdot \text{diagram}_8 \\
& + \frac{1}{6} \cdot \text{diagram}_9 + \frac{1}{6} \cdot \text{diagram}_{10} + \frac{1}{6} \cdot \text{diagram}_{11} + \frac{1}{6} \cdot \text{diagram}_{12} + \frac{1}{6} \cdot \text{diagram}_{13} + \frac{1}{6} \cdot \text{diagram}_{14} \\
& + \dots
\end{aligned} \tag{20}$$

The + and – signs adjacent to the grey line in each diagram here indicate the side on which the set of + and – vertices is located. As one can see, there are cuts intercepting more than one propagator. In the following, a cut going through r propagators will be called a “ r -particle cut”.

It is important to note that cut vacuum-vacuum diagrams would be zero in the vacuum because energy cannot flow from from one side of the cut to the other in the absence of external legs. This constraint is removed if the fields are coupled to **time-dependent** external sources. Thus, in this case, cut vacuum-vacuum diagrams, and therefore the imaginary part of vacuum-vacuum diagrams, differ from zero.

3.2 Probability of producing n particles

All transition amplitudes contain the factor $\exp(i\mathcal{V}[j])$, which, in the squared amplitudes, transforms to the factor $\exp(-2 \operatorname{Im} \mathcal{V}[j])$. The power counting rules derived earlier tell us that the sum of all the connected vacuum-vacuum diagrams starts at order⁶ g^{-2} . Hence, we will write

$$i(\mathcal{V}[j] - \mathcal{V}^*[j]) = 2 \operatorname{Im} \mathcal{V}[j] \equiv \frac{a}{g^2}, \tag{21}$$

where a denotes a series in g^{2n} that starts at order $n = 0$; the coefficients of this series are functions of gj . Thus, the vacuum-to-vacuum transition probability is $\exp(-a/g^2)$. The simplest tree diagrams entering in a/g^2 were displayed in eq. (20).

We now turn to the probabilities for producing n particles. For now, our discussion is more intuitive than rigorous, with precise definitions to be introduced later in the section (in 3.5). Besides the overall factor $\exp(i\mathcal{V}[j])$, the transition amplitude from the vacuum state to a state containing one particle is the sum of all the Feynman diagrams with one external line. These diagrams

⁶From now on, we shall not write explicitly the dependence in the combination gj because we shall assume the fields are strong and this combination is of order unity. All the coefficients in the expressions we write in this section depend implicitly on gj .

start at order g^{-1} . The probability to produce one particle from the vacuum can therefore be parameterized as

$$P_1 = e^{-a/g^2} \frac{b_1}{g^2}, \quad (22)$$

where b_1 is, like a , a series in g^{2n} that starts at $n = 0$. b_1/g^2 can be obtained by performing a 1-particle cut through vacuum-vacuum diagrams. In other words, b_1/g^2 is one of the contributions that one can find in a/g^2 . Diagrammatically, b_1/g^2 starts at tree level with

$$\begin{aligned} \frac{b_1}{g^2} = & \frac{1}{2} \begin{array}{c} \bullet \\ | \\ \bullet \end{array} + \frac{1}{2} \begin{array}{c} \bullet \\ | \\ \bullet \end{array} \\ & + \frac{1}{6} \begin{array}{c} \bullet \\ | \\ \bullet \end{array} + \frac{1}{6} \begin{array}{c} \bullet \\ | \\ \bullet \end{array} + \frac{1}{6} \begin{array}{c} \bullet \\ | \\ \bullet \end{array} + \frac{1}{6} \begin{array}{c} \bullet \\ | \\ \bullet \end{array} + \frac{1}{6} \begin{array}{c} \bullet \\ | \\ \bullet \end{array} + \frac{1}{6} \begin{array}{c} \bullet \\ | \\ \bullet \end{array} \\ & + \dots \end{aligned} \quad (23)$$

Consider now the probability P_2 for producing two particles from the vacuum. There is an obvious contribution to this probability that is obtained simply by squaring the b_1/g^2 piece of the probability for producing one particle. This term corresponds to the case where the two particles are produced independently from one another. But two particles can also be produced correlated to each other. This “correlated” contribution to P_2 must come from a 2-particle cut through connected vacuum-vacuum diagrams. Let us represent this quantity as b_2/g^2 . Diagrammatically, b_2/g^2 is a series whose first terms are

$$\begin{aligned} \frac{b_2}{g^2} = & \frac{1}{6} \begin{array}{c} \bullet \\ | \\ \bullet \end{array} + \frac{1}{6} \begin{array}{c} \bullet \\ | \\ \bullet \end{array} + \frac{1}{6} \begin{array}{c} \bullet \\ | \\ \bullet \end{array} + \frac{1}{6} \begin{array}{c} \bullet \\ | \\ \bullet \end{array} + \frac{1}{6} \begin{array}{c} \bullet \\ | \\ \bullet \end{array} + \frac{1}{6} \begin{array}{c} \bullet \\ | \\ \bullet \end{array} \\ & + \dots \end{aligned} \quad (24)$$

The net probability, from correlated and uncorrelated production, of two particles can therefore be represented as

$$P_2 = e^{-a/g^2} \left[\frac{1}{2!} \frac{b_1^2}{g^4} + \frac{b_2}{g^2} \right] .. \quad (25)$$

The prefactor $1/2!$ in front of the first term is a symmetry factor which is required because the two particles in the final state are undistinguishable.

Let us further discuss the case of three particle production before proceeding to the general case. One (“uncorrelated”) term will be the cube of b_1/g^2 (preceded by a symmetry factor $1/3!$). A combination $b_1 b_2/g^4$ will also appear, corresponding to the case where two of the particles are produced in the same subdiagram, and the third is produced independently. Finally, there is an “intrinsic” three particle production probability corresponding to the three particles produced in the same diagram. We shall represent this contribution

by b_3/g^2 . More precisely, b_3/g^2 is the sum of all 3-particle cuts in a/g^2 . Diagrammatically, some of the simplest terms in b_3/g^2 are

$$\frac{b_3}{g^2} = \frac{1}{8} \text{[diagram 1]} + \frac{1}{8} \text{[diagram 2]} + \frac{1}{8} \text{[diagram 3]} + \dots \quad (26)$$

(Only a few terms have been represented at this order, due to the large number of possible permutations of cuts across the various legs.) The probability of producing three particles from the vacuum is then given by

$$P_3 = e^{-a/g^2} \left[\frac{1}{3!} \frac{b_3^3}{g^6} + \frac{b_1 b_2}{g^4} + \frac{b_3}{g^2} \right]. \quad (27)$$

The previous examples can be generalized to obtain an expression for the production of n particles, for any n . It reads

$$P_n = e^{-a/g^2} \sum_{p=0}^n \frac{1}{p!} \sum_{\alpha_1 + \dots + \alpha_p = n} \frac{b_{\alpha_1} \dots b_{\alpha_p}}{g^{2p}}. \quad (28)$$

In this formula, p is the number of disconnected subdiagrams producing the n particles, and b_r/g^2 denotes the contribution to the probability of the sum of all r -particle cuts through the connected vacuum-vacuum diagrams. This formula gives the probability of producing n particles to all orders in the coupling g in a field theory with strong external sources⁷. To the best of our knowledge, this formula is new. Even though the dynamical details are not specified, its compact analytical form can be used to derive very general results for multi-particle production. These results will be discussed extensively in the section on AGK rules. Indeed, their generality follows from the fact that the dynamical details are not specified. A more rigorous derivation of this formula is presented in section 3.5.

3.3 Unitarity

In our framework, the statement of unitarity is simply that the sum of the probabilities P_n be unity, namely,

$$\sum_{n=0}^{\infty} P_n = 1. \quad (29)$$

From eq. (28), it is a simple matter of algebra to show that the l.h.s. above is given by

$$\sum_{n=0}^{\infty} P_n = e^{-a/g^2} \exp \left[\frac{1}{g^2} \sum_{r=1}^{\infty} b_r \right]. \quad (30)$$

⁷Recall also that, in addition to the factors of g^2 that appear explicitly in the formula, the terms a, b_r are series in g^{2n} where, further, the coefficients of the series are functions of $g_j \sim 1$

Unitarity therefore requires that

$$a = \sum_{r=1}^{\infty} b_r . \quad (31)$$

This relationship between a and the b_r 's is in fact an identity following directly from their respective definitions. Indeed, recall that (see eq. (21)) a/g^2 is equal to twice the imaginary part of the sum of connected vacuum-vacuum diagrams. Therefore, a/g^2 is the sum of all the possible cuts through these connected vacuum-vacuum diagrams. On the other hand, b_r/g^2 was defined as the subset of cut vacuum-vacuum diagrams with r -particle cuts. (Recall that these are cuts that intercept r propagators.) The sum of these over all values of r is therefore equal to a/g^2 by definition. Eq. (31) therefore confirms that the identity in eq. (20) is precisely the unitarity condition.

3.4 Moments of the distribution

Moments of the distribution of probabilities P_n are easily computed with the generating function

$$F(x) \equiv \sum_{n=0}^{\infty} P_n e^{nx} , \quad (32)$$

such that $\langle n^p \rangle = F^{(p)}(0)$. Using eq. (28), this generating function can be evaluated in closed form, and one obtains

$$F(x) = e^{-a/g^2} \exp \left[\frac{1}{g^2} \sum_{r=1}^{\infty} b_r e^{rx} \right] = \exp \left[\frac{1}{g^2} \sum_{r=1}^{\infty} b_r (e^{rx} - 1) \right] . \quad (33)$$

The mean of the distribution of multiplicities, $\langle n \rangle \equiv \sum_n n P_n$, is

$$\langle n \rangle = F'(0) = \frac{1}{g^2} \sum_{r=1}^{\infty} r b_r . \quad (34)$$

The average multiplicity is therefore given by the sum of all r -particle cuts through the connected vacuum-vacuum diagrams, weighted by the number r of particles on the cut. The second derivative of $F(x)$ at $x = 0$ is simply

$$F''(0) = \langle n^2 \rangle . \quad (35)$$

The variance of the distribution, $\sigma \equiv \langle n^2 \rangle - \langle n \rangle^2$, can instead be obtained directly from the second derivative of

$$G(x) \equiv \ln F(x) = \frac{1}{g^2} \sum_{r=1}^{\infty} b_r (e^{rx} - 1) \quad (36)$$

at $x = 0$. Thus,

$$\sigma = G''(0) = \frac{1}{g^2} \sum_{r=1}^{\infty} r^2 b_r . \quad (37)$$

More generally, the connected part of the moment of order p reads

$$\langle n^p \rangle_{\text{connected}} = G^{(p)}(0) = \frac{1}{g^2} \sum_{r=1}^{\infty} r^p b_r . \quad (38)$$

One sees that if $b_r \neq 0$ for at least one $r > 1$, the variance and the mean are not equal and the distribution is not a Poisson distribution. The converse is true: it is trivial to check that eq. (28) is a Poisson distribution if $b_1 \neq 0$ and $b_r = 0$ for $r > 1$. Indeed, in this case, eq. (28) would simply be

$$P_n = e^{-b_1/g^2} \frac{1}{n!} \left(\frac{b_1}{g^2} \right)^n . \quad (39)$$

In a certain sense, eq. (28) is approximately Poissonian, since the term $(b_1/g^2)^n$ has the largest power of g^{-2} in P_n . However, even if this approximation is a good one for the individual probabilities P_n , it leads to an error of relative order unity for the value of the mean multiplicity; eq. (39) gives $\langle n \rangle = b_1/g^2$, while the correct value is $\langle n \rangle = g^{-2} \sum_r r b_r$.

3.5 Formal derivation of eq. (28)

In section 3.2, the probabilities P_n for producing n particles were expressed in terms of b_r/g^2 . The latter are the r -particle cuts in the sum of cut connected vacuum-vacuum diagrams. We worked out the expressions for P_n in terms of b_r only for the cases $n = 1, 2, 3$ and guessed a generalization of the formula to an arbitrary n . We shall here derive more rigorously this expression for P_n and shall rewrite it formally to identify the b_r coefficients.

An important step in the forthcoming proof is to note that the expectation value of the time ordered product of n fields is

$$\langle 0_{\text{out}} | T \phi(x_1) \cdots \phi(x_n) | 0_{\text{in}} \rangle = \frac{\delta}{i\delta j(x_1)} \cdots \frac{\delta}{i\delta j(x_n)} e^{i\mathcal{V}[j]} . \quad (40)$$

This formula is equivalent to the usual way of obtaining time-ordered Green's functions from a generating functional. However, in our case, the source j is not a fictitious variable that one sets to zero at the end but is instead the (physical) external source. We can also use the standard LSZ reduction formula [48] to rewrite the amplitude for producing n particles as ⁸

$$\langle \mathbf{p}_1 \cdots \mathbf{p}_n \text{out} | 0_{\text{in}} \rangle = \frac{1}{Z^{n/2}} \int \left[\prod_{i=1}^n d^4 x_i e^{ip_i \cdot x_i} (\square_{x_i} + m^2) \frac{\delta}{i\delta j(x_i)} \right] e^{i\mathcal{V}[j]} . \quad (41)$$

⁸The wave-function renormalization factors Z correspond to self-energy corrections on the cut propagators of the vacuum-vacuum diagrams.

The probability for producing n -particles is given by the expression

$$P_n = \frac{1}{n!} \int \left[\prod_{i=1}^n \frac{d^3 \mathbf{p}_i}{(2\pi)^3 2E_i} \right] |\langle \mathbf{p}_1 \cdots \mathbf{p}_{n \text{out}} | 0_{\text{in}} \rangle|^2, \quad (42)$$

where $E_i \equiv \sqrt{\mathbf{p}_i^2 + m^2}$. Substituting the r.h.s. of eq. (41) in the above, and noting that

$$G_{+-}^0(x, y) = \int \frac{d^3 \mathbf{p}_i}{(2\pi)^3 2E_i} e^{i\mathbf{p} \cdot (x-y)}, \quad (43)$$

is the Fourier transform of the expression in eq. (17), we can write the probability P_n directly as

$$P_n = \frac{1}{n!} \mathcal{D}^n[j_+, j_-] e^{i\mathcal{V}[j_+]} e^{-i\mathcal{V}^*[j_-]} \Big|_{j_+=j_-=j}, \quad (44)$$

where $\mathcal{D}[j_+, j_-]$ is the operator

$$\mathcal{D}[j_+, j_-] \equiv \frac{1}{Z} \int d^4x d^4y G_{+-}^0(x, y) (\square_x + m^2)(\square_y + m^2) \frac{\delta}{\delta j_+(x)} \frac{\delta}{\delta j_-(y)}. \quad (45)$$

The sources in the amplitude and the complex conjugate amplitude are labeled as j_+ and j_- respectively to ensure that the functional derivatives act only on one of the two factors.

In eq. (44), the mass m in G_{+-}^0 and in $\square + m^2$ is the physical pole mass of the particles under consideration rather than their bare mass. The role of the prefactor Z^{-1} becomes more transparent if we write

$$\mathcal{D} = \int d^4x d^4y Z G_{+-}^0(x, y) \frac{\square_x + m^2}{Z} \frac{\square_y + m^2}{Z} \frac{\delta}{\delta j_+(x)} \frac{\delta}{\delta j_-(y)}, \quad (46)$$

and recall that Z is the residue of the pole of the renormalized propagator. All the factors under the integral in eq. (46) are therefore renormalized propagators, or their inverse.

Using eq. (44), we can write the generating function $F(x)$, defined earlier in eq. (32), as

$$F(x) = e^{e^x \mathcal{D}[j_+, j_-]} e^{i\mathcal{V}[j_+]} e^{-i\mathcal{V}^*[j_-]} \Big|_{j_+=j_-=j}. \quad (47)$$

The reader may note that the factor $\exp(i\mathcal{V}[j_+])$ represents the sum of the usual Feynman vacuum-vacuum diagrams with source j_+ . Likewise, the factor $\exp(-i\mathcal{V}^*[j_-])$ is comprised of the complex conjugate of vacuum-vacuum diagrams, with source j_- . One thus begins to see a formal realization of the intuitive discussion of the previous section in terms of cut diagrams. Alternately, the second factor of eq. (47) can be interpreted as containing terms in the Schwinger-Keldysh expansion [50,51] that have only $+$ vertices, while the third factor contains terms that have only $-$ vertices. A brief introduction to the Schwinger-Keldysh formalism is provided in appendix A.

We shall now further elaborate on the interpretation of P_n (and $F(x)$) as cut vacuum-vacuum Feynman diagrams as well as their relation to the Schwinger-Keldysh framework. Consider the action of the operator $\mathcal{D}[j_+, j_-]$ on the vacuum-vacuum factors in eq. (47). The operator $Z^{-1}(\square_x + m^2)\delta/\delta j_+(x)$ takes a diagram of $\exp(i\mathcal{V}[j_+])$, removes one of its sources, and amputates the propagator to which this source was attached. (This procedure includes any self-energy decoration on this propagator because of the factor Z^{-1} .) $Z^{-1}(\square_y + m^2)\delta/\delta j_-(y)$ does the same on the factor $\exp(-i\mathcal{V}^*[j_-])$. Finally, the factor $ZG_{+-}^0(x, y)$ is a (dressed) propagator that links the two diagrams that have been opened by the functional derivatives with respect to the sources. When $x = 0$, one can convince oneself that the action of the operator $\exp(\mathcal{D}[j_+, j_-])$ is to build all the other vacuum-vacuum diagrams of the Schwinger-Keldysh formalism, namely those that have at least one G_{-+}^0 or G_{+-}^0 ,

$$e^{\mathcal{D}[j_+, j_-]} e^{i\mathcal{V}[j_+]} e^{-i\mathcal{V}^*[j_-]} = e^{i\mathcal{V}_{SK}[j_+, j_-]} . \quad (48)$$

Here $i\mathcal{V}_{SK}[j_+, j_-]$ denotes the sum of all connected vacuum-vacuum diagrams in the Schwinger-Keldysh formalism, with the source j_+ on the upper branch of the contour and likewise, j_- on the lower branch. When the magnitudes of the sources on the upper and lower branches are the same, $j_+ = j_- = j$, it is well known that this sum of all vacuum-vacuum diagrams is equal to 1. (This statement is proved in appendix A.) Therefore, eq. (47) satisfies $F(0) = 1$, as unitarity dictates it should.

When $x \neq 0$, the generating function $F(x)$ is the sum of all vacuum-vacuum diagrams in the Schwinger-Keldysh formalism, with the two ‘‘off-diagonal’’ propagators substituted by

$$\begin{aligned} G_{-+}^0 &\rightarrow e^x G_{-+}^0 , \\ G_{+-}^0 &\rightarrow e^x G_{+-}^0 , \end{aligned} \quad (49)$$

and where the source is the same on the upper and lower branches of the contour. Naturally, the logarithm of this generating function is obtained by keeping only the connected vacuum-vacuum diagrams in the sum.

Recall now that the building blocks of the Schwinger-Keldysh perturbative expansion are the same as those obtained by the cutting rules for calculating the imaginary parts of Feynman diagrams. We can therefore identify each term in the expansion of $F(x)$ with a cut vacuum-vacuum diagram. Moreover, one sees from eq. (49) that the power of e^x in a given term is equal to the number of propagators G_{-+}^0 or G_{+-}^0 it contains. Therefore, the order in e^x equals the number of particles on the cut. Since $\ln(F(x))$ contains only the cut **connected** vacuum-vacuum diagrams, and since b_r/g^2 has been defined earlier as the sum of all the r -particle cuts through connected vacuum-vacuum diagrams, we have just proved that

$$\ln(F(x)) = -\frac{a}{g^2} + \sum_{r=1}^{\infty} e^{rx} \frac{b_r}{g^2} . \quad (50)$$

The coefficients b_r can thus be formally identified and computed in principle. One obtains the constant term in this formula, $-a/g^2$, from the limit $x \rightarrow -\infty$ of eq. (47) and from eq. (21).

4 Direct calculation of the average multiplicity

In the previous section, we obtained a general expression for a generating function which can be used, in principle, to compute all moments of the multiplicity distribution. In this section, we will concentrate on the first moment, the average multiplicity. We will develop the Schwinger-Keldysh formalism, introduced previously in section 3.5 and in appendix A, to compute this quantity both at leading and next-to-leading order. While the result at leading order is well known, the next-to-leading order result is new, and is the central result of this paper.

4.1 General formula

Although one could in principle compute the average multiplicity using eq. (34), it would be extremely impractical because this method requires one to evaluate separately all the r -particle cuts through the vacuum-vacuum diagrams⁹. It is much more straightforward to obtain the multiplicity from the generating function given in eq. (47). We obtain

$$\langle n \rangle = F'(0) = \mathcal{D}[j_+, j_-] \left. e^{i\mathcal{V}_{SK}[j_+, j_-]} \right|_{j_+ = j_- = j}, \quad (51)$$

where we have used eq. (48). Writing out $\mathcal{D}[j_+, j_-]$ explicitly using eq. (45), this expression can be rewritten as

$$\begin{aligned} \langle n \rangle = \int d^4x d^4y Z G_{+-}^0(x, y) \frac{\square_x + m^2}{Z} \frac{\square_y + m^2}{Z} \\ \times \left[\frac{\delta i\mathcal{V}_{SK}}{\delta j_+(x)} \frac{\delta i\mathcal{V}_{SK}}{\delta j_-(y)} + \frac{\delta i\mathcal{V}_{SK}}{\delta j_+(x)\delta j_-(y)} \right]_{j_+ = j_- = j} \quad .. \quad (52) \end{aligned}$$

Functional derivatives of the sum of connected vacuum-vacuum diagrams are connected Green's functions with the number of external points equalling the number of derivatives. When we differentiate $i\mathcal{V}_{SK}$,

$$\frac{\delta}{\delta j_{\epsilon_1}(x_1)} \cdots \frac{\delta}{\delta j_{\epsilon_n}(x_n)} i\mathcal{V}_{SK}[j_+, j_-] = \langle 0_{\text{in}} | P \phi^{(\epsilon_1)}(x_1) \cdots \phi^{(\epsilon_n)}(x_n) | 0_{\text{in}} \rangle_{\text{conn}}, \quad (53)$$

the corresponding Green's functions are the path-ordered Green's functions defined in eq. (113) of appendix A. More precisely, they are the connected components of these Green's functions – hence the subscript “conn”. The operators

⁹This would be an almost impossible task even at tree level.

$Z^{-1}(\square + m^2)$ in eq. (52) amputate the external legs of these Green's functions (along with the self-energy corrections they may carry).

Denoting $\Gamma^{(\epsilon_1 \dots \epsilon_n)}(x_1, \dots, x_n)$ as the amputated version of the Green's function in eq. (53), we finally express the average multiplicity as¹⁰

$$\langle n \rangle = \int d^4x d^4y ZG_{+-}^0(x, y) \left[\Gamma^{(+)}(x)\Gamma^{(-)}(y) + \Gamma^{(+)}(x, y) \right]_{j_+=j_-=j}. \quad (56)$$

This formula is valid to all orders in the coupling constant and is a key result of this paper as will become clearer later. Diagrammatically, we can represent it as

$$\langle n \rangle = \text{Diagram 1} + \text{Diagram 2}, \quad (57)$$

where the shaded blobs represent the amputated Green's functions Γ . In principle, one should amputate as well the self-energy corrections attached to their external points and use the full $-+$ propagator. Alternatively, one can use the bare $-+$ propagator, and keep the self-energy corrections attached to the external legs of the shaded blobs.

Since the Γ 's are connected Green's functions, the second of the two diagrams is at least a 1-loop diagram. Therefore only the first diagram can contribute at leading order in the coupling. The functions Γ are obtained with the standard Schwinger-Keldysh rules, described in the appendix A. Note also that, unlike the expressions for the probabilities, there are no vacuum-vacuum diagrams left in this formula. They have all disappeared thanks to the fact that $\exp(i\mathcal{V}_{SK}[j, j]) = 1$. This makes the evaluation of the multiplicity much simpler than that of the probabilities P_n even for $n = 1$.

4.2 Leading order result

The multiplicity at leading order, namely $\mathcal{O}(g^{-2}(gj)^n)$, is obtained from the left diagram in eq. (57) with each of the two blobs evaluated at tree level. We have,

$$\langle n \rangle_{LO} = \sum_{+/-} \text{Diagram 3}, \quad (58)$$

¹⁰If one is only interested in the calculation of the multiplicity $\langle n \rangle$, a more elementary derivation is to start from

$$\langle n \rangle = \int \frac{d^3\mathbf{p}}{(2\pi)^3 2E_p} \langle 0_{\text{in}} | a_{\text{out}}^\dagger(\mathbf{p}) a_{\text{out}}(\mathbf{p}) | 0_{\text{in}} \rangle. \quad (54)$$

A reduction formula for the correlator that appears under the integral gives

$$\begin{aligned} \langle 0_{\text{in}} | a_{\text{out}}^\dagger(\mathbf{p}) a_{\text{out}}(\mathbf{p}) | 0_{\text{in}} \rangle &= \frac{1}{Z} \int d^4x d^4y e^{-ip \cdot x} e^{ip \cdot y} \\ &\quad \times (\square_x + m^2)(\square_y + m^2) \langle 0_{\text{in}} | \phi(x)\phi(y) | 0_{\text{in}} \rangle. \end{aligned} \quad (55)$$

The expectation value on the right hand side, in which the fields are not time-ordered, is just the propagator $G_{-+}(x, y)$ of the Schwinger-Keldysh formalism. Splitting it into connected and disconnected contributions, one can see that eqs. (54)-(55) and (56) are equivalent.

where the sum is over all the tree diagrams on the left and on the right of the propagator G_{+-}^0 (represented in boldface) as well as a sum over the labels $+/-$ of the vertices whose type is not written explicitly. At this order, the mass in G_{+-}^0 is simply the bare mass, and $Z = 1$.

Eq. (58) can be expressed very simply in terms of the **retarded** solutions of the classical equations of motion. The identities,

$$\begin{aligned} G_{++}^0 - G_{+-}^0 &= G_R^0, \\ G_{-+}^0 - G_{--}^0 &= G_R^0, \end{aligned} \quad (59)$$

where G_R^0 is the free retarded propagator, will be essential in demonstrating this result. Consider for instance, one of the tree subdiagrams contained in eq. (58). Summing over the $+$ or $-$ indices of the “leaves” (or “blobs”) of the tree, the outer layer of propagators is transformed into retarded propagators, thanks to eqs. (59). These then give factors of $\int d^4y G_R(\dots, y)j(y)$ that are independent of the indices of the vertices immediately below. This trick is applicable here because the source $j(x)$ is identical on both branches of the closed time path. By repeating this procedure recursively until one reaches the “root” of the tree, one turns all the propagators into retarded propagators. As a consequence, one finally obtains the same tree diagram (ending at point x or y), where all the propagators are now retarded propagators.

Now recall the perturbative expansion of the retarded solution of the classical equation of motion¹¹

$$(\square + m^2)\phi_c(x) + \frac{g}{2}\phi_c^2(x) = j(x), \quad (60)$$

with an initial condition at $x_0 = -\infty$ such that the field and its derivatives vanish

$$\lim_{x^0 \rightarrow -\infty} \phi_c(x) = 0, \quad \lim_{x^0 \rightarrow -\infty} \partial^\mu \phi_c(x) = 0. \quad (61)$$

In that case as well, the solution can be expressed, identically, recursively, in terms of the retarded Green’s function.

The sum over all leaves up to the root of the tree on each side of the cut in eq. (58) can therefore be identified as

$$\phi_c(x) = \sum_{+/-} \overset{x}{+} \text{---} \begin{array}{c} \bullet \\ \diagup \quad \diagdown \\ \text{---} \quad \text{---} \\ \bullet \quad \bullet \end{array} = \sum_{+/-} \overset{x}{-} \text{---} \begin{array}{c} \bullet \\ \diagup \quad \diagdown \\ \text{---} \quad \text{---} \\ \bullet \quad \bullet \end{array}. \quad (62)$$

Note that in eq. (58), we need to amputate these tree diagrams, so it is $(\square + m^2)\phi_c(x)$ that enters in eq. (58) rather than $\phi_c(x)$ itself. More precisely, we have

$$\langle n \rangle_{LO} = \int d^4x d^4y G_{+-}^0(x, y) (\square_x + m^2)(\square_y + m^2) \phi_c(x) \phi_c(y). \quad (63)$$

¹¹To see that the various factors of i present in the Feynman rules of the Schwinger-Keldysh formalism agree with this identification, simply multiply eq. (60) by i , and recall that we have defined the propagators as the inverse of $i(\square + m^2)$ – for instance, see eq. (17).

Using the explicit momentum space form for G_{+-}^0 in eq. (43), we can rewrite

$$\langle n \rangle_{LO} = \int \frac{d^3 \mathbf{p}}{(2\pi)^3 2E_p} \left| \int d^4 x e^{ip \cdot x} (\square + m^2) \phi_c(x) \right|^2. \quad (64)$$

This leading order result is well known. In the CGC framework for gluon production, the multiplicity was evaluated by computing the spatial Fourier transform of the classical field ϕ_c at late times [26,27,30,31,33,34]. To connect their work to our eq. (64), we use the identity

$$e^{ip \cdot x} (\partial_0^2 + E_p^2) \phi_c(x) = \partial_0 (e^{ip \cdot x} [\partial_0 - iE_p] \phi_c(x)), \quad (65)$$

and perform an integration by parts of the r.h.s. of eq. (64) (using the initial condition of eq. (61)) to obtain

$$\int d^4 x e^{ip \cdot x} (\square + m^2) \phi_c(x) = \lim_{x^0 \rightarrow +\infty} \int d^3 \mathbf{x} e^{ip \cdot x} [\partial_{x_0} - iE_p] \phi_c(x). \quad (66)$$

In practice, the r.h.s. of this equation is the preferred method for evaluating the average multiplicity. One only needs to solve the classical equation of motion with the initial conditions of eq. (61) and perform a spatial Fourier transform of the solution at the latest time.

4.3 Next-to-leading order result

At next-to-leading order (NLO) in the coupling constant ($\mathcal{O}(g^0(gj)^n)$), one obtains two sorts of corrections to the leading contribution of eq. (58):

- (i) the right diagram in eq. (57) with the blob evaluated at tree level


(67)

- (ii) 1-loop corrections to diagrams of the kind displayed in eq. (58). These come from the left diagram of eq. (57), with one of the blobs evaluated at 1 loop, and the other blob kept at tree level


(68)

In both cases, these contributions provide corrections of order g^0 to the multiplicity $\langle n \rangle$, to be compared to the leading contributions of order g^{-2} .

That one obtains these two sets of contributions at NLO is also well known. However, what is novel, and will be demonstrated below, is that both these contributions can be computed entirely with retarded boundary conditions and retarded propagators. *This makes it feasible to perform NLO computations (to all orders in the external sources) by solving equations of motion for the classical and small fluctuation fields with boundary conditions entirely specified at $t = -\infty$.*

4.3.1 Evaluation of eq. (67)

We begin by discussing the diagrams displayed in eq. (67). These topologies are well known since they are the ones involved for the production of fermion-antifermion pairs [55]. (Indeed, for this process, they constitute the lowest order contribution.) Evaluating the diagrams of eq. (67) is equivalent to calculating the tree level propagator G_{+-} attached to an arbitrary number of tree diagrams of the type depicted in eq. (62). Each of these attachments, thanks to eq. (62), can be replaced by the classical field ϕ_c itself. Thus

$$\sum_{+/-} \begin{array}{c} \bullet \\ \bullet \\ \bullet \\ \bullet \\ \bullet \\ \text{---} \\ \bullet \\ \bullet \\ \bullet \end{array} \begin{array}{c} x \\ + \\ \text{---} \\ \text{---} \\ \text{---} \\ y \\ - \end{array} = \sum_{+/-} \begin{array}{c} \circ \\ \text{---} \\ \text{---} \\ \text{---} \\ \text{---} \\ y \\ - \end{array}, \quad (69)$$

where a dotted line terminating in a cross represents an insertion of the classical field (eq. (62)). At the vertices where ϕ_c 's are inserted, the $+/-$ indices must still be summed over; a vertex of type $-$ simply corresponds to a sign change for the field insertion. This is equivalent to computing the propagator $G_{+-}(x, y)$ in the presence of the background field ϕ_c . We shall mimic the method used in [55] and write down a Lippmann-Schwinger equation whose solution is $G_{+-}(x, y)$. For later reference, we shall write it for any component $G_{\epsilon\epsilon'}(x, y)$ as

$$G_{\epsilon\epsilon'}(x, y) = G_{\epsilon\epsilon'}^0(x, y) - ig \sum_{\eta, \eta'=\pm} \int d^4z G_{\epsilon\eta}^0(x, z) \phi_c(z) \sigma_{\eta\eta'}^3 G_{\eta'\epsilon'}(z, y), \quad (70)$$

where the resummed propagator has no superscript 0. $\sigma^3 = \text{diag}(1, -1)$ is the third Pauli matrix, and its purpose in eq. (70) is to provide the correct minus sign when the vertex at which the classical field is inserted is of type $-$.

The Lippmann-Schwinger equation is solved by performing a simple rotation¹² of the $+/-$ indices. The details of this procedure can be followed in appendix B. The solution of the Lippmann-Schwinger equation for the ‘‘rotated’’ propagator \mathbf{G} reads

$$\mathbf{G} = \begin{pmatrix} 0 & G_A \\ G_R & G_S \end{pmatrix}, \quad (71)$$

¹²Such transformations were introduced in [56] and discussed more systematically in [57].

where the resummed retarded and advanced propagators are given by

$$G_R = G_R^0 \sum_{n=0}^{\infty} [\phi_c G_R^0]^n, \quad G_A = G_A^0 \sum_{n=0}^{\infty} [\phi_c G_A^0]^n, \quad (72)$$

and

$$G_S = G_R (G_R^0)^{-1} G_S^0 (G_A^0)^{-1} G_A. \quad (73)$$

Here G_R^0 and G_A^0 are the free retarded and advanced propagators respectively, and $G_S^0 = G_{++}^0 + G_{--}^0 \equiv 2\pi\delta(p^2 - m^2)$. The combination $G_R G_R^0^{-1}$ is the full retarded propagator in the presence of the background field ϕ_c , amputated of its rightmost leg. The propagators $G_{\epsilon\epsilon'}$ of the Schwinger-Keldysh formalism are obtained by performing the inverse of the rotations described in appendix B and the explicit expressions are given there.

To compute the next-to-leading order contribution to the multiplicity $\langle n \rangle$ from eq. (67), we need specifically the propagator G_{+-} . The solution of the Lippman-Schwinger equation gives

$$G_{+-} = G_R G_R^0{}^{-1} G_{+-}^0 G_A^0{}^{-1} G_A \quad (74)$$

We are not done yet because eq. (56) tells us that one has to amputate the external legs of G_{+-} . This requirement is conveniently fulfilled by introducing “retarded and advanced scattering T-matrices”, defined by the relations

$$\begin{aligned} G_R &\equiv G_R^0 + G_R^0 T_R G_R^0, \\ G_A &\equiv G_A^0 + G_A^0 T_A G_A^0. \end{aligned} \quad (75)$$

The contribution of eq. (67) to $\langle n \rangle$ is then given by

$$\langle n \rangle_{NLO}^{(1)} = \int \frac{d^3\mathbf{p}}{(2\pi)^3 2E_p} \int d^4x d^4y e^{-ip \cdot x} e^{ip \cdot y} \int d^4u d^4v T_R(x, u) G_{+-}^0(u-v) T_A(v, y). \quad (76)$$

In momentum space, it reads more compactly as

$$\langle n \rangle_{NLO}^{(1)} = \int \frac{d^3\mathbf{p}}{(2\pi)^3 2E_p} \int \frac{d^3\mathbf{q}}{(2\pi)^3 2E_q} T_R(p, -q) T_A(-q, p). \quad (77)$$

Using the identity that $T_A(-q, p) = [T_R(p, -q)]^*$, we obtain finally,

$$\langle n \rangle_{NLO}^{(1)} = \int \frac{d^3\mathbf{p}}{(2\pi)^3 2E_p} \int \frac{d^3\mathbf{q}}{(2\pi)^3 2E_q} |T_R(p, -q)|^2. \quad (78)$$

This formula is the equivalent for scalar bosons of eq. (50) in [55] and eq. (94) in [58].

The retarded T -matrix $T_R(p, -q)$ can be computed from the retarded solution of the partial differential equation¹³,

$$(\square + m^2 + g\phi_c(x))\eta(x) = 0, \quad (79)$$

¹³We remind the reader that g is a dimensionful quantity.

where η is a small perturbation about the classical background field ϕ_c ; the equation is therefore the linearized equation of motion in this background. Using Green's theorem¹⁴ (see appendix A of [59] for an extended discussion),

$$\eta(x) = i \int_{y_0=\text{const}} d^3 \vec{y} G_R(x, y) \overset{\leftrightarrow}{\partial}_{y_0} \eta(y), \quad (80)$$

as well as eq. (75), one can prove that

$$T_R(p, -q) = \lim_{x_0 \rightarrow +\infty} \int d^3 \mathbf{x} e^{ip \cdot x} [\partial_{x_0} - iE_p] \eta(x), \quad (81)$$

where $\eta(x)$ is the retarded solution of eq. (79) with initial condition $\eta(x) = e^{iq \cdot x}$ when $x_0 \rightarrow -\infty$. One should not confuse this equation with eq. (66), despite the fact that they look similar. When using eq. (66) one must solve the classical equation of motion in the presence of the source j in order to obtain ϕ_c . In eq. (81), one is instead solving the equation of motion for a perturbation η about the classical solution ϕ_c . The eigenvalues of this perturbation are used to construct the small fluctuations propagator in the background field. The analog of eq. (81) for fermion production was previously used in [58] and [36,37] to evaluate the yield of quark-antiquark pairs in pA collisions and in the initial stages of nucleus-nucleus collisions respectively.

4.3.2 Evaluation of eq. (68)

We will now consider NLO contributions to the multiplicity from 1-loop corrections such as those depicted in eq. (68). Only the subdiagram that contains a closed loop is new. Using the same trick as in eq. (66), the contribution of eq. (68) to $\langle n \rangle_{NLO}$ can be written as

$$\begin{aligned} \langle n \rangle_{NLO}^{(2)} &= \int \frac{d^3 \mathbf{p}}{(2\pi)^3 2E_p} \left[\lim_{x_0 \rightarrow +\infty} \int d^3 \mathbf{x} e^{ip \cdot x} [\partial_0 - iE_p] \phi_c(x) \right] \\ &\quad \times \left[\lim_{x_0 \rightarrow +\infty} \int d^3 \mathbf{x} e^{ip \cdot x} [\partial_0 - iE_p] \phi_{c,1}(x) \right]^* + \text{c.c.} \end{aligned} \quad (82)$$

The novel quantity considered here is the 1-loop correction to $\phi_c(x)$ – we will represent this quantity as $\phi_{c,1}(x)$. We will discuss below our strategy to compute this quantity by solving partial differential equations with boundary conditions at $x^0 \rightarrow -\infty$.

All the diagrams contributing to $\phi_{c,1}(x)$ include a closed loop, to which may be attached an arbitrary number of tree diagrams. All but one of these tree diagrams are terminated by sources j ; this last one has an external leg at the

¹⁴The prefactor i is due to the fact that the inverse of $\square + m^2$ is iG according to our conventions for the propagators.

point x ,

$$\phi_{c,1}(x) = \sum_{+/-} \frac{x}{+} \text{ [diagram of a central circle with multiple legs, each ending in a tree structure of vertices and edges] } \quad (83)$$

The first simplification one can perform is to use eq. (62) to collapse all the trees terminated by sources into insertions of the classical field ϕ_c . This gives

$$\phi_{c,1}(x) = \sum_{+/-} \frac{x}{+} \text{ [diagram of a central circle with a single leg leading to point x, and several vertices on the leg and circle, each with a small circle containing a plus sign] } \quad (84)$$

Again, at each remaining vertex or insertion of ϕ_c , one must sum over the type $+/-$. The number of insertions of ϕ_c can be arbitrary, both on the loop and on the leg leading to the final point x . Therefore, eq. (84) can be written more explicitly as

$$\phi_{c,1}(x) = -ig \sum_{\epsilon=\pm} \epsilon \int d^4y G_{+\epsilon}(x,y) G_{\epsilon\epsilon}(y,y), \quad (85)$$

where all the propagators in this formula must be evaluated in the presence of the background field ϕ_c .

We can rewrite $\phi_{c,1}$ as ¹⁵

$$\begin{aligned} \phi_{c,1}(x) &= -ig \int d^4y G_{++}(y,y) \sum_{\epsilon=\pm} \epsilon G_{+\epsilon}(x,y) \\ &= -ig \int d^4y G_R(x,y) G_{++}(y,y), \end{aligned} \quad (87)$$

where we have used eq. (59). This expression is equivalent to the *retarded* solution of the following partial differential equation:

$$(\square + m^2 + g\phi_c(x))\phi_{c,1}(x) = -g G_{++}(x,x), \quad (88)$$

¹⁵From eqs. (123) of appendix B, we see that the propagators $G_{++}(y,y)$ and $G_{--}(y,y)$, which enter in eq. (85), are both equal to

$$G_{++}(y,y) = G_{--}(y,y) = \frac{1}{2} G_R^0 G_R^{-1} G_S^0 G_A^{-1} G_A. \quad (86)$$

with an initial condition such that $\phi_{c,1}$ and its derivatives vanish at $x_0 = -\infty$. The source term $G_{++}(x, x)$ in eq. (88) is given by eq. (86),

$$\begin{aligned} G_{++}(x, x) &= \frac{1}{2} \int d^4u d^4v \left[G_R G_R^{0-1} \right](x, u) G_S^0(u, v) \left[G_A^{0-1} G_A \right](v, x) \\ &= \frac{1}{2} \int \frac{d^4q}{(2\pi)^4} 2\pi\delta(q^2 - m^2) \int d^4u \left[G_R G_R^{0-1} \right](x, u) e^{iq \cdot u} \\ &\quad \times \int d^4v \left[G_A^{0-1} G_A \right](v, x) e^{-iq \cdot v}, \quad (89) \end{aligned}$$

using

$$G_S^0(u, v) = \int \frac{d^4q}{(2\pi)^4} e^{iq \cdot (u-v)} 2\pi\delta(q^2 - m^2). \quad (90)$$

From the r.h.s. of the relation,

$$\int d^4u \left[G_R G_R^{0-1} \right](x, u) e^{iq \cdot u} = \lim_{u_0 \rightarrow -\infty} i \int d^3\mathbf{u} G_R(x, u) \overset{\leftrightarrow}{\partial}_{u_0} e^{iq \cdot u} \equiv \eta(x), \quad (91)$$

we see that this quantity is precisely the retarded solution at point x of eq. (79) with an initial condition $\eta(u) = e^{iq \cdot u}$ at $u_0 = -\infty$. Further, by noticing that

$$\left[G_A^{0-1} G_A \right](v, x) = \left[G_R G_R^{0-1} \right](x, v), \quad (92)$$

the factor involving $G_A^{0-1} G_A$ in eq. (89) is obtained in a similar way, except that the initial condition must be $e^{-iq \cdot v}$.

Following this discussion, we can now outline here an algorithm for obtaining the quantity $\phi_{c,1}(x)$ needed in the calculation of $\langle n \rangle_{NLO}^{(2)}$:

- (i) For an arbitrary on-shell momentum q , find the solutions $\eta_q^{(+)}(x)$ and $\eta_q^{(-)}(x)$ of eq. (79) whose initial conditions at $x_0 \rightarrow -\infty$ are respectively $\eta_q^{(+)}(x) = e^{iq \cdot x}$ and $\eta_q^{(-)}(x) = e^{-iq \cdot x}$
- (ii) Calculate $G_{++}(x, x)$ as

$$G_{++}(x, x) = \frac{1}{2} \int \frac{d^4q}{(2\pi)^4} 2\pi\delta(q^2 - m^2) \eta_q^{(+)}(x) \eta_q^{(-)}(x). \quad (93)$$

- (iii) Solve eq. (88) with a vanishing initial condition at $x_0 = -\infty$

For completeness, we note that $G_{++}(x, x)$ contains ultraviolet divergences. They appear as a divergence in the integration over the momentum q in eq. (93). By going back to the diagrams that are contained in $G_{++}(x, x)$, it is easy to see that these divergences are the usual 1-loop ultraviolet divergences of the ϕ^3 field theory in the vacuum, namely, the tadpole and the self-energy divergences¹⁶.

¹⁶Of course, the scalar toy model with a ϕ^3 self-interaction that we are considering in this paper is somewhat peculiar in the ultraviolet sector, since this theory is super-renormalizable in four dimensions. But the procedure outlined here for removing the divergences would be valid in QCD as well.

These divergences correspond to the two terms of eq. (84) in which the loop is dressed by zero or one insertions of the classical field ϕ_c (the terms with two insertions of ϕ_c or more on the loop involve the 1-loop corrections to the n -point functions for $n \geq 3$, which are finite in four dimensions). From this observation, it is clear that one must subtract the following quantity from $G_{++}(x, x)$

$$\delta G_{++}(x, x) \equiv \delta_1 + (\delta_z \square + \delta_{m^2}) \phi_c(x), \quad (94)$$

where δ_1 is the counterterm that makes the tadpole finite, and δ_z and δ_{m^2} the two counterterms that make the self-energy finite. One possible approach is to evaluate both eq. (93) and the counterterms with the same momentum cutoff Λ , and to subtract eq. (94) from eq. (93) before letting Λ go to infinity.

5 AGK cancellations

We will discuss here a set of combinatorial rules that relate the discussions of the n -particle probabilities in section 3 and the average multiplicity in the previous section. We find that these combinatorial relations are identical to the Abramovsky–Gribov–Kancheli (AGK) cancellations first discussed [39] in the context of reggeon field theory. This enables us to map out explicitly, in the context of multi-particle production, the terminology of field theories with external sources (such as the Color Glass Condensate) with that of reggeon field theory. Our discussion is in fact more general than the original AGK discussion, since it is not limited to diagrams that have an interpretation in terms of reggeons alone.

Before we proceed, we shall provide here a very brief sketch of the extensive literature on the subject of the AGK cutting rules. A review of early work can be found in ref. [40]. Applications of AGK rules to reggeon field theory models of particle production in proton-nucleus and nucleus-nucleus collisions were discussed at length by Koplik and Mueller [41]. More recently, several authors considered the application of these rules in perturbative QCD. For a comprehensive recent discussion, see Ref. [42,43] and references therein. We note that AGK rules have also been considered previously in the Mueller dipole picture [44] of saturation/CGC [45,46]. A detailed discussion and additional references can be found in [47].

5.1 AGK-like identities

The AGK relations are a set of identities that relate the average multiplicity of particles produced in hadronic collisions to the multiplicity of a single cut reggeon. Thanks to these identities, all the other contributions to the average multiplicity involving more than one reggeon exchange (where the reggeons that are not cut correspond to absorptive corrections) cancel in the calculation of the average multiplicity.

Even though our discussion is based on a completely different theory, one can obtain a set of identities that play the same role as the original AGK identities¹⁷. To see these, consider $P_{n,m}$, the term that has a factor $1/g^{2m}$ in the expression eq. (28) for P_n ,

$$P_{n,m} = \frac{1}{g^{2m}} \sum_{p+q=m} \frac{(-a)^q}{q!} \frac{1}{p!} \sum_{\alpha_1+\dots+\alpha_p=n} b_{\alpha_1} \dots b_{\alpha_p} \dots \quad (95)$$

Obviously one has

$$P_n = \sum_{m=0}^{\infty} P_{n,m} . \quad (96)$$

Here m is the number of disconnected subdiagrams contributing to P_n ; each disconnected diagram starts at order g^{-2} . In eq. (95), q is the number of disconnected subdiagrams that are not cut – they do not contribute to the number n of produced particles, and correspond to the “absorptive corrections” of [39]. Likewise, p is the number of subdiagrams that are cut – they contribute to the number of produced particles. In the model of [39], m would be the number of reggeons in the diagram.

There is however one important difference between our considerations and those of [39]. In our paper, n is the number of produced **particles**, while in [39] n is the number of **cut reggeons**, regardless of how many particles are produced in each of them. Therefore, in our case, n can be larger than m (because each cut subdiagram can produce many particles), while n is always smaller or equal to m in [39].

We shall now introduce the term of order $1/g^{2m}$, $F_m(x)$, in the generating function $F(x)$ introduced in section 3. It is defined as

$$F_m(x) \equiv \sum_{n=0}^{\infty} P_{n,m} e^{nx} = \frac{1}{m!} \frac{1}{g^{2m}} \left(\sum_{r=0}^{\infty} b_r e^{rx} - a \right)^m . \quad (97)$$

This formula can be obtained either by using eq. (95) and performing the sum explicitly, or by expanding eq. (33) to the appropriate order $1/g^{2m}$. Evaluating the successive derivatives of $F_m(x)$ at $x = 0$, we can easily prove the identities

$$\begin{aligned} \text{if } m \geq 2 , \quad & \sum_{n=1}^{\infty} n P_{n,m} = 0 , \\ \text{if } m \geq 3 , \quad & \sum_{n=2}^{\infty} n(n-1) P_{n,m} = 0 , \\ \dots & \end{aligned} \quad (98)$$

To prove these formulas, we used the unitarity relation, $a = \sum_r b_r$. The physical interpretation of these formulas is quite transparent. They tell us that Feynman

¹⁷In this sense, one can understand these identities to be a very general consequence of field theories with strong external sources.

diagrams that have two or more disconnected subdiagrams do not affect the mean multiplicity, that Feynman diagrams with three or more disconnected subdiagrams do not affect the variance, and so on... These identities are the generalization to our situation of the eqs. (24) of [39].

Note that the sum over n must be extended to infinity due to the above mentioned fact that we are counting particles instead of cut reggeons.

5.2 Closer connection with reggeon theory

One can in fact make more detailed connections with the discussion of ref. [39], and in a sense, generalize the results there. Recall that the latter is formulated in the language of reggeons so the connections to our framework are not obvious. We remind the reader that in eq. (28), for P_n , the index p represents the number of cut subdiagrams contributing to the production of the n particles. Therefore, one can further divide P_n and write the probability for having an event in which n particles are produced in p cut subdiagrams¹⁸

$$P_{n,p}^{(c)} = e^{-a/g^2} \frac{1}{p!} \sum_{\alpha_1 + \dots + \alpha_p = n} \frac{b_{\alpha_1} \dots b_{\alpha_p}}{g^{2p}}, \quad (99)$$

which of course is related to P_n by

$$P_n = \sum_{p=0}^n P_{n,p}^{(c)}. \quad (100)$$

The unspecified ‘‘subdiagrams’’ in our discussion are a generalization of the ‘‘reggeons’’ of [39]. Since the discussion in [39] was at the level of the cut reggeons rather than at the level of the individual particles, we may obtain a closer correspondence to the results in [39] by integrating out the index n representing the number of produced particles. Summing over n in eq. (99) gives the probability of having p cut subdiagrams,

$$\mathcal{R}_p \equiv \sum_{n=p}^{+\infty} P_{n,p}^{(c)} = \frac{1}{p!} \left(\frac{a}{g^2} \right)^p e^{-a/g^2}. \quad (101)$$

Clearly, the multiplicity of cut subdiagrams has a Poissonian distribution. This is not a surprise because they are disconnected from one another¹⁹. Moreover, the average number of cut subdiagrams is equal to

$$\langle n_{\text{cut}} \rangle \equiv \sum_{p=0}^{+\infty} p \mathcal{R}_p = \frac{a}{g^2}. \quad (102)$$

¹⁸This new quantity $P_{n,p}^{(c)}$ should not be confused with $P_{n,m}$. The latter is the probability for producing n particles in m subdiagrams, irrespective of whether cut or uncut. Defining $P_{n,p,q}$ as the probability of producing n particles with p cut subdiagrams and q uncut subdiagrams, the former quantities are respectively $P_{n,m} = \sum_{p+q=m} P_{n,p,q}$ and $P_n^{(c)} = \sum_{q=0}^{+\infty} P_{n,p,q}$.

¹⁹In [39], this result was achieved thanks to an assumption about the impact factors, while in our model it follows naturally because particle production arises only through the coupling to an external source.

One may define the average number of particles produced in diagrams with p cut subdiagrams as²⁰

$$\langle n \rangle_p \equiv \frac{\sum_{n=p}^{+\infty} n \mathcal{P}_{n,p}^{(c)}}{\sum_{n=p}^{+\infty} \mathcal{P}_{n,p}^{(c)}} = p \frac{\sum_{r=1}^{+\infty} r b_r}{a}. \quad (103)$$

This result implies that

$$\langle n \rangle_p = p \langle n \rangle_1. \quad (104)$$

In other words, a diagram with p cut subdiagrams produces on average p times the number of particles produced by a diagram with a single cut subdiagram. Further, one can deduce immediately that the average number of produced particles, $\langle n \rangle = g^{-2} \sum_r r b_r$, is the average number of cut subdiagrams multiplied by the average number of particles produced in one cut subdiagram,

$$\langle n \rangle = \langle n_{\text{cut}} \rangle \langle n \rangle_1. \quad (105)$$

This property was assumed in ref. [39]; they therefore focused only on properties of the distribution of cut reggeons. In our approach, this property arises naturally, regardless of the nature of the subdiagrams we consider. (This result is therefore more general than the ladder diagrams that correspond to reggeons.)

In order to exactly reproduce the identities in [39], we introduce the probability $\mathcal{R}_{p,m}$ of having p cut subdiagrams for a total number m of subdiagrams ($m - p$ of which are therefore uncut). Expanding the exponential in eq. (101) to order $m - p$, one obtains

$$\mathcal{R}_{p,m} = \frac{1}{(m-p)!} \frac{1}{p!} \left(-\frac{a}{g^2} \right)^{m-p} \left(\frac{a}{g^2} \right)^p. \quad (106)$$

This distribution of probabilities then satisfies the relations

$$\begin{aligned} \text{if } m \geq 2, \quad & \sum_{p=1}^m p \mathcal{R}_{p,m} = 0, \\ \text{if } m \geq 3, \quad & \sum_{p=2}^m p(p-1) \mathcal{R}_{p,m} = 0, \\ \dots & \end{aligned} \quad (107)$$

This set of identities is strictly equivalent to the eqs. (24) of [39]. For instance, the first relation means that diagrams with two or more subdiagrams cancel in the calculation of the multiplicity. These relations are therefore a straightforward consequence of the fact that the distribution of the numbers of cut subdiagrams is a Poisson distribution. They do not depend at all on whether

²⁰This quantity must be defined as a conditional probability. Indeed, the denominator is necessary in this definition in order to take into account the fact that events with different numbers of cut subdiagrams can occur with different probabilities.

these subdiagrams are “reggeons” or not. In appendix C, we prove the reverse result: the only distribution \mathcal{R}_p for which eqs. (107) hold is a Poisson distribution.

It is also instructive to note that these identities obeyed by the distribution of cut/uncut disconnected subdiagrams have been obtained by “integrating out” the number n of produced particles. By doing so, one goes from the distribution (99) – which still depends on all the quantities $b_1, b_2, b_3 \dots$ – to (101), in which all the dynamics is summarized in one number $a = \sum_r b_r$. Integrating out the number of particles has the virtue of hiding most of the details of the field theory under consideration. This is in fact the reason why the AGK identities have a range of validity which is much wider than the reggeons models for which they had been derived originally.

However, this robustness has a cost: by integrating out the number of particles, one has lost a lot of information about the details of the theory, which means that certain questions can no longer be addressed. For instance, in eq. (104), the factor $\langle n \rangle_1$ – the average number of particles produced in one cut subdiagram – can only be calculated by going back to the microscopic dynamics of the theory under consideration.

5.3 Additional cancellations in $\langle n \rangle$

In the original approach of Abramovsky, Gribov and Kancheli, one would estimate the particle multiplicity predicted by the reggeon model as follows:

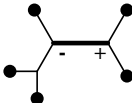
- (i) compute the diagram with one cut reggeon exchange in order to obtain the average number of cut reggeons, $\langle n_{\text{cut}} \rangle$
- (ii) calculate the average number of particles in one cut reggeon $\langle n \rangle_1$. This second step in general requires a more microscopic description of what one means by “reggeons”

The advantage of our approach is of course that it is entirely formulated as a field theory in which the elementary objects are particles. This makes it possible to compute these two quantities from first principles. Indeed, expressions for these in terms of cuts through vacuum-vacuum Feynman diagrams are

$$\langle n_{\text{cut}} \rangle = \frac{a}{g^2}, \quad \langle n \rangle_1 = \frac{g^{-2} \sum_r r b_r}{a g^{-2}}. \quad (108)$$

As one can see, in our microscopic description, there is a further cancellation in their product, between $\langle n_{\text{cut}} \rangle$ and the denominator of $\langle n \rangle_1$. This result could be anticipated because we already know that the average multiplicity is equal to $g^{-2} \sum_r r b_r$.

Moreover, by comparing eqs. (34) and (58), we see that we have the following identity at leading order,

$$\frac{1}{g^2} \sum_{r=1}^{\infty} r b_r|_{LO} = \sum \text{Diagram} \quad (109)$$


In the r.h.s. of this relation, the types of the endpoints of the propagator represented in boldface must be held fixed, and one must sum over the topologies and over the $+/-$ indices for the trees on both sides of this propagator. The diagrammatic expansion of the left hand side of eq. (109) is of course obtained from eqs. (23), (24), (26), etc... We also know from eq. (62) that the tree diagrams that appear in the r.h.s. are nothing but the retarded solution of the classical equation of motion. In other words, eq. (109) tells us that the sum of all cuts through (**time-ordered**) tree connected vacuum-vacuum diagrams, weighted by the particle multiplicity on the cut, can be cast into a much simpler expression in terms of **retarded** tree diagrams. This means that additional cancellations must occur in the left hand side of eq. (109) in order to have this dramatic simplification. These cancellations are discussed explicitly in appendix D.

5.4 Higher moments

The cancellations discussed in the previous subsection, which are in fact responsible for the identity of eq. (109), are crucial in order to be able to calculate the particle multiplicity in a simple way. We have seen explicitly that one can calculate the multiplicity at leading order directly from the classical field ϕ_c , and in principle at higher orders as well. Of course, the NLO calculation has the complications of a typical 1-loop calculation; in particular one has to treat the ultraviolet divergences.

It turns out that higher moments of the multiplicity distribution are also calculable from ϕ_c , by formulas that are tractable even though they are more complicated than in the case of the multiplicity. Let us consider the case of the variance as an illustration. It is obtained as the second derivative at $x = 0$ of the log of the generating function, $\ln(F(x))$. Therefore, it is given by

$$\sigma \equiv \langle n^2 \rangle - \langle n \rangle^2 = [\mathcal{D}[j_+, j_-] + \mathcal{D}^2[j_+, j_-]] e^{i\mathcal{V}_{SK}[j_+, j_-]} \Big|_{\substack{j_+ = j_- = j \\ \text{connected}}} . \quad (110)$$

Performing the functional derivatives and dropping the disconnected terms that show up gives

$$\begin{aligned} \sigma = \langle n \rangle + \int d^4x d^4y d^4u d^4v G_{+-}^0(x, y) G_{+-}^0(u, v) & \left[\Gamma^{(+-+-)}(x, y, u, v) \right. \\ & + \Gamma^{(-++)}(y, u, v) \Gamma^{(+)}(x) + \Gamma^{(++-)}(x, u, v) \Gamma^{(-)}(y) + (x \leftrightarrow u, y \leftrightarrow v) \\ & + \Gamma^{(++)}(x, u) \Gamma^{(--)}(y, v) + \Gamma^{(+-)}(x, v) \Gamma^{(-+)}(y, u) \\ & + \Gamma^{(+-)}(x, v) \Gamma^{(-)}(y) \Gamma^{(+)}(u) + \Gamma^{(-+)}(y, u) \Gamma^{(+)}(x) \Gamma^{(-)}(v) \\ & \left. + \Gamma^{(++)}(x, u) \Gamma^{(-)}(y) \Gamma^{(-)}(v) + \Gamma^{(--)}(y, v) \Gamma^{(+)}(x) \Gamma^{(+)}(u) \right], \quad (111) \end{aligned}$$

where the Γ 's are amputated Green's functions in the Schwinger-Keldysh for-

malism. Diagrammatically, the variance can be expressed as

$$\begin{aligned}
\sigma = \langle n \rangle + & \text{ (tree level diagrams) } + 2 \text{ (1-loop diagrams) } + 2 \text{ (2-loop diagrams) } \\
& + \text{ (1-loop diagrams) } + \text{ (2-loop diagrams) } \\
& + \text{ (2-loop diagrams) }
\end{aligned} \tag{112}$$

All the diagrams represented in this equation are deviations from a Poisson distribution (for which we would simply have $\sigma = \langle n \rangle$). The diagrams of the first line start at tree level, while those of the second and third lines start respectively at 1 and 2 loops. Similar formulas can be derived for even higher moments, but they become increasingly complicated as the order of the moment increases, even at tree level.

6 Summary and Outlook

In this paper, we studied particle production in a model ϕ^3 scalar field theory coupled to a strong ($j \sim 1/g$) time dependent external source. This theory is a toy model of the Color Glass Condensate formalism for particle production in high energy hadronic collisions in QCD. We shall summarize here some of the novel results of this paper.

- We obtained a general formula (eq. (28)) for the probability P_n to produce n particles in a field theory with time dependent external sources. (A formal expression of this formula is given in eqs. (44) and (45).)
- We derived the corresponding generation function for moments of the multiplicity distribution. We showed that the generating function (eq. (47)) can be related to the sum of all vacuum-vacuum diagrams in the Schwinger-Keldysh formalism with off-diagonal propagators given by eq. (49).
- We obtained a general formula (eq. (56)) for the average particle multiplicity in terms of the amputated Schwinger-Keldysh Green's functions. While the result to leading order is well known, the result at next-to-leading order (NLO) is new and remarkable. It is not surprising of course that the average multiplicity at NLO can be expressed in terms of small fluctuation fields. What is non-trivial and remarkable is that these fields can be computed by solving small fluctuation equations of motion with *retarded* propagators and initial conditions specified at $x^0 \rightarrow -\infty$ (eqs. (79), (88) and (93)).
- We outlined an algorithm to compute these NLO contributions. Such an algorithm has been implemented previously for fermion pair production in

the Color Glass Condensate, where the diagram of eq. (67) is the leading contribution. It has not been implemented for the diagram of eq. (68).

- We observed that the Abramovsky-Gribov-Kancheli cancellations, originally formulated in terms of relations among reggeon diagrams, can be mapped into the field theory language of cut vacuum-vacuum diagrams. Disconnected vacuum-vacuum subgraphs can be identified as reggeons and corresponding cut sub-graphs as cut reggeons.
- We showed that an immediate consequence of this mapping is that AGK cancellations in reggeon field theory hold if and only if the distribution of cut reggeons is Poissonian. This follows because two disconnected cut sub-diagrams do not interact by definition! The conjecture is proved explicitly in appendix C. We observed that there are additional cancellations (as represented by eq. (109)) that are not visible at the level of the AGK cancellations.
- We derived a general formula for the second moment (the variance) of the multiplicity distribution. This formula can be expressed in terms of the average multiplicity plus “non-Poissonian” terms. These are nonzero even at tree level in a field theory with strong time dependent external sources.

We shall now discuss some of the ramifications of our results, in particular for high energy QCD. Our studies were indeed motivated by their possible relevance to hadronic collisions at very high energies. In particular, in the Color Glass Condensate approach, hadronic collisions at very high energies are described by an effective field theory where the degrees of freedom are wee parton fields coupled to strong time dependent external valence sources. A key feature of the CGC approach is that weak coupling techniques are applicable. The techniques developed here can therefore be applied to study particle production²¹. Of particular interest is particle production in the earliest stages of heavy ion collisions, and the possibility that one can understand the thermalization of a quark gluon plasma from first principles. As is immediately clear from the formalism developed here, the solution of such problems is intrinsically non-perturbative (even in weak coupling) requiring the summation of infinite series of Feynman graphs. Numerical algorithms performing these summations are therefore essential.

Indeed, first steps in carrying out the program outlined here have already been performed. Gluon production [29,30,31,32,33,34] and quark pair production [36,37] have been computed numerically previously to leading order in the coupling and to all orders in the source density. There are strong hints that a deeper understanding of thermalization requires an analysis incorporating energy loss effects [61,62,63]. These may include the scattering contributions of the bottom-up scenario [64,65], or equivalently the energy loss induced by collective effects [66,67,68]. In the CGC framework, these effects can be shown to appear

²¹However, one should keep in mind the fact that transition amplitudes in a slowly varying background might be difficult to define rigorously [60].

at next-to-leading order in the coupling. Qualitative studies [69,35] of the NLO effects suggest that these may be very important in driving the system towards equilibrium. Our study here is a first step towards a quantitative formulation of this problem. In a follow up study [70], we will address the connections of our approach to kinetic approaches [71,72].

Acknowledgements

We thank Robi Peschanski, Jochen Bartels and George Sterman for enlightening discussions on the AGK rules, Sangyong Jeon for useful discussions during the early stages of this work, and our colleagues at Saclay and Brookhaven and Keijo Kajantie for many discussions on related topics. RV's research was supported by DOE Contract No. DE-AC02-98CH10886. FG wishes to thank the hospitality of TIFR, Mumbai, and the support of CEPIPRA project No 3104-3.

A Schwinger-Keldysh formalism

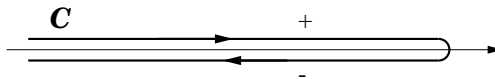


Figure 1: The closed time path used in the Schwinger-Keldysh formalism.

Our intuitive discussion of cutting rules for computing probabilities in field theories coupled to external sources, begun in section 2.3 and continuing in section 3, culminates in the formal expression of these, in section 3.5, in terms of the Schwinger-Keldysh vacuum-vacuum amplitudes. The Schwinger-Keldysh formalism was developed in the 1960's in the context of many-body quantum field theory [50,51]. It is used primarily in thermal field theory problems in order to calculate thermal averages of operators [73]. Since it may be less familiar to those working outside this area, we will provide a brief review of the formalism before proceeding to prove a result stated in section 3.5.

The primary feature of the Schwinger-Keldysh formalism, relative to the standard formulation of quantum field theory, is that the time flow of paths is defined on a contour comprised of two branches (see the figure 1) wrapping the real axis. The upper branch, denoted $+$, runs along the real axis in the positive direction while the lower branch, denoted $-$, runs in the opposite direction. The aim is to compute the correlation functions

$$G^{\{\epsilon_1 \dots \epsilon_n\}}(x_1 \dots x_n) \equiv \langle 0_{\text{in}} | P_{\mathcal{C}} \phi^{(\epsilon_1)}(x_1) \dots \phi^{(\epsilon_n)}(x_n) | 0_{\text{in}} \rangle, \quad (113)$$

where $P_{\mathcal{C}}$ denotes a path ordering of operators along the time contour. Operators are ordered from left to right by decreasing values of their curvilinear abscissa on the contour, with operators living on the lower branch placed to the left of

operators living on the upper branch. When restricted to the upper branch, it is equivalent to the usual time ordering. Similarly, it is equivalent to an anti-time ordering on the lower branch. In eq. (113), the indices ϵ_i can have the values $+/-$ indicating the branch of the contour where the corresponding field is located. This definition of the path ordering suggests that the correlator defined in eq. (113) can also be written as

$$G^{\{\epsilon_1 \dots \epsilon_n\}}(x_1 \dots x_n) = \langle 0_{\text{in}} | \overline{T} \left[\prod_{i|\epsilon_i=-} \phi^{(\epsilon_i)}(x_i) \right] T \left[\prod_{j|\epsilon_j=+} \phi^{(\epsilon_j)}(x_j) \right] | 0_{\text{in}} \rangle. \quad (114)$$

Note that the vacuum state used in order to define this correlation function is the “in” vacuum state on both sides²².

The perturbative calculation of the correlator in eq. (113) requires special Feynman rules. These are obtained in the Schwinger-Keldysh formalism and their derivation is analogous to that of regular time-ordered correlation functions. One first expresses the Heisenberg fields in terms of the free field ϕ_{in} of the interaction picture. One can then rewrite eq. (113) as

$$G^{\{\epsilon_1 \dots \epsilon_n\}}(x_1 \dots x_n) = \langle 0_{\text{in}} | P_{\mathcal{C}} \phi_{\text{in}}^{(\epsilon_1)}(x_1) \dots \phi_{\text{in}}^{(\epsilon_n)}(x_n) e^{\int_{\mathcal{C}} d^4x \mathcal{L}_{\text{int}}(\phi_{\text{in}}(x))} | 0_{\text{in}} \rangle. \quad (115)$$

Note that the time integration in the exponential now runs over the full contour \mathcal{C} . The perturbative expansion of this correlator is obtained by expanding the exponential. This procedure differs from the usual Feynman rules in the following two ways:

- at each vertex, the time integration runs over the full contour \mathcal{C}
- the free propagator connecting vertices is the path-ordered product of two free fields

$$G^0(x, y) \equiv \langle 0_{\text{in}} | P_{\mathcal{C}} \phi_{\text{in}}(x) \phi_{\text{in}}(y) | 0_{\text{in}} \rangle. \quad (116)$$

These rules are implemented by first breaking the time integration at each vertex in two pieces. One corresponds to an integration over times in the upper branch while the other integrates over the lower branch. The vertices come in two varieties, $+$ vertices and $-$ vertices, and the indices must be summed over at each vertex. For example, the contribution of the $-$ vertices is written as an integration over the real axis in the positive direction modulo the addition of a minus sign to the vertex of type $-$. This follows from the fact that the integration runs in the negative direction on the lower branch of \mathcal{C} . Likewise, the propagator in eq. (116) is broken into four different propagators, corresponding to where the two fields lie on the contour \mathcal{C} ,

$$\begin{aligned} G_{++}^0(x, y) &\equiv \langle 0_{\text{in}} | T \phi_{\text{in}}(x) \phi_{\text{in}}(y) | 0_{\text{in}} \rangle, \\ G_{--}^0(x, y) &\equiv \langle 0_{\text{in}} | \overline{T} \phi_{\text{in}}(x) \phi_{\text{in}}(y) | 0_{\text{in}} \rangle, \\ G_{-+}^0(x, y) &\equiv \langle 0_{\text{in}} | \phi_{\text{in}}(x) \phi_{\text{in}}(y) | 0_{\text{in}} \rangle, \\ G_{+-}^0(x, y) &\equiv \langle 0_{\text{in}} | \phi_{\text{in}}(y) \phi_{\text{in}}(x) | 0_{\text{in}} \rangle. \end{aligned} \quad (117)$$

²²This feature is a consequence of the fact that the thermal average of an operator is a **trace** of the operator multiplied by the density matrix.

Note that the Fourier transforms of these free propagators are precisely those encountered previous in the derivation of cutting rules (see eq. (17)). The propagator $G_{\epsilon\epsilon'}^0$ connects a vertex of type ϵ to a vertex of type ϵ' .

In the discussion in section 3.1, the \pm vertices, propagators and sources were introduced as a formal trick to compute the sum of the Feynman vacuum-vacuum amplitude and its complex conjugate amplitude. We now understand these as arising naturally from the Schwinger-Keldysh formalism which captures the physics of theories in external fields/finite temperatures. For example, an identity (eq. (16)) that we showed in section 3.1 is equivalent to a property of the Schwinger-Keldysh formalism used in section 3.5: *the sum of all vacuum-vacuum diagrams is equal to one*. It remains true even if the field is coupled to an external source, provided that source is the same on the upper and lower branches of the contour \mathcal{C} .

The proof of this result in the Schwinger-Keldysh formalism is very simple. Consider a connected vacuum-vacuum diagram, and integrate out all but one of its vertices. The result is a function of a single point we call x . This function, by virtue of not possessing external legs, and being coupled to a source that has the same value on the $+$ and $-$ branches of the contour, has the same magnitude on both branches of the contour. Therefore, when we sum over the $+/-$ type of this last vertex, we get an exact cancellation because the $-$ index has the opposite sign and the same magnitude as $+$ index. Thus all **connected** vacuum-vacuum diagrams are zero when the sources are identical on both legs of the contour. Because the sum of **all** vacuum-vacuum diagrams, is the exponential of the sum of the connected ones, it is therefore equal to unity.

B Solution of Lippman-Schwinger equation

The Lippman-Schwinger equation (70) can be solved by performing the following rotations of the propagators and field insertions:

$$\begin{aligned} G_{\epsilon\epsilon'} &\rightarrow \mathbf{G}_{\alpha\beta} \equiv \sum_{\epsilon,\epsilon'=\pm} U_{\alpha\epsilon} U_{\beta\epsilon'} G_{\epsilon\epsilon'} \\ \boldsymbol{\sigma}_{\epsilon\epsilon'}^3 &\rightarrow \boldsymbol{\Sigma}_{\alpha\beta}^3 \equiv \sum_{\epsilon,\epsilon'=\pm} U_{\alpha\epsilon} U_{\beta\epsilon'} \boldsymbol{\sigma}_{\epsilon\epsilon'}^3 \end{aligned} \quad (118)$$

with

$$U = \frac{1}{\sqrt{2}} \begin{pmatrix} 1 & -1 \\ 1 & 1 \end{pmatrix}. \quad (119)$$

Under these rotations, the free matrix propagator and field insertion matrix become

$$\mathbf{G}_{\alpha\beta}^0 = \begin{pmatrix} 0 & G_A^0 \\ G_R^0 & G_S^0 \end{pmatrix}, \quad \boldsymbol{\Sigma}_{\alpha\beta}^3 = \begin{pmatrix} 0 & 1 \\ 1 & 0 \end{pmatrix}. \quad (120)$$

G_R^0 and G_A^0 are the free retarded and advanced propagators, and G_S^0 stands for the combination

$$G_S^0 \equiv G_{++}^0 + G_{--}^0. \quad (121)$$

Its Fourier transform is $G_s^0(p) = 2\pi\delta(p^2 - m^2)$. In terms of these new propagators and vertices, the Lippmann-Schwinger equation has the same form as that of eq. (70), modulo the replacements of eq. (118). The main simplification follows from observing that the product $\mathbf{G}\Sigma^3$ is the sum of a diagonal matrix and a nilpotent matrix. This makes it easy to calculate its n -th power. In particular, we have²³

$$\mathbf{G}^0 [\Sigma^3 \mathbf{G}^0]^n = \begin{pmatrix} 0 & [G_A^0]^{n+1} \\ [G_R^0]^{n+1} & \sum_{i=0}^n [G_R^0]^i G_s^0 [G_A^0]^{n-i} \end{pmatrix}. \quad (122)$$

Note that the off-diagonal equations mean that in the new basis the Lippmann-Schwinger equations do not mix the retarded and advanced propagators.

The result above can be easily inverted to obtain the propagators of the Schwinger-Keldysh formalism. One obtains²⁴

$$\begin{aligned} G_{-+} &= G_R G_R^{0-1} G_{-+}^0 G_A^{0-1} G_A \\ G_{+-} &= G_R G_R^{0-1} G_{+-}^0 G_A^{0-1} G_A \\ G_{++} &= \frac{1}{2} [G_R G_R^{0-1} G_s^0 G_A^{0-1} G_A + (G_R + G_A)] \\ G_{--} &= \frac{1}{2} [G_R G_R^{0-1} G_s^0 G_A^{0-1} G_A - (G_R + G_A)] . \end{aligned} \quad (123)$$

As one can see, all these propagators resumming the effect of the classical background field ϕ_c can be expressed in terms of the retarded and advanced propagator in the background field. This is a useful property because retarded propagators can be obtained by solving a simple partial differential equation with retarded boundary conditions. (Advanced propagators can be obtained from the retarded ones by permuting the endpoints.)

C Reciprocal of eqs. (107)

It is also instructive to see what the AGK identities, as given in eqs. (107), imply for the distribution of multiplicities of cut subdiagrams in eq. (101). Let us assume the following generic form for the probability \mathcal{R}_p of having p cut subdiagrams :

$$\mathcal{R}_p \equiv R(\eta) \frac{1}{p!} r_p \eta^p, \quad (124)$$

²³This formula is true even if each propagator has different arguments. Therefore, it is also true for the convolution of $n + 1$ propagators, between which one inserts the classical field.

²⁴One can check that this solution satisfies the following properties

$$\begin{aligned} G_{++} + G_{--} &= G_{-+} + G_{+-} \\ G_{++} - G_{+-} &= G_R, \quad G_{++} - G_{-+} = G_A . \end{aligned}$$

where η is a parameter that counts the number of subdiagrams (in the situation studied in section 5.2, the quantity a/g^2 played this role). The prefactor $R(\eta)$ is determined from the requirement that the sum of these probabilities be unity,

$$R(\eta) = \left[\sum_{p=0}^{+\infty} \frac{1}{p!} r_p \eta^p \right]^{-1}, \quad (125)$$

and the coefficients r_p must be positive in order to have positive probabilities. Moreover, we can assume without loss of generality that $r_0 = 1$. The $\mathcal{R}_{p,q}$ that appear in eqs. (107) are obtained by expanding the prefactor $R(\eta)$ to order $q-p$, and are thus completely determined from the coefficients r_p .

The relations (107) are very complicated non-linear relations when expressed in terms of the coefficients r_p , because of the prefactor $R(\eta)$. In order to investigate their consequences, it is much easier to introduce the function

$$G(x) \equiv \sum_{p=0}^{+\infty} \frac{1}{p!} r_p (\eta x)^p. \quad (126)$$

Note that the prefactor $R(\eta)$ is nothing but $G^{-1}(1)$. Therefore, if we consider the following generating function for the probabilities \mathcal{R}_p ,

$$H(x) \equiv \sum_{p=0}^{+\infty} \mathcal{R}_p x^p, \quad (127)$$

it is related to $G(x)$ via :

$$H(x) = G(x)/G(1). \quad (128)$$

Recalling now that

$$\mathcal{R}_p = \sum_{q=p}^{+\infty} \mathcal{R}_{p,q}, \quad (129)$$

and using eqs. (107), we have the following relations for the successive derivatives of $H(x)$ at $x = 1$:

$$H^{(1)}(1) = \mathcal{R}_{1,1}, \quad H^{(2)}(1) = 2! \mathcal{R}_{2,2}, \quad \dots \quad H^{(p)}(1) = p! \mathcal{R}_{p,p}. \quad (130)$$

Therefore, we can rewrite the generating function $H(x)$ as

$$H(x) = \sum_{p=0}^{+\infty} \mathcal{R}_{p,p} (x-1)^p = \sum_{p=0}^{+\infty} \frac{1}{p!} r_p (x-1)^p = G(x-1). \quad (131)$$

In order to obtain the second equality, we have used the fact that $\mathcal{R}_{p,p}$ is obtained by keeping only the order 0 in the expansion of the prefactor $R(\eta)$, which is equal to unity from our choice to have $r_0 = 1$. Therefore, the AGK identities, eqs. (107), imply that

$$\forall x, \quad G(x) = G(x-1)G(1). \quad (132)$$

One sees immediately that the exponentials, $G(x) = \exp(\alpha x)$, are trivial solutions of this functional relation. Note that this solution corresponds to a Poisson distribution for the probabilities \mathcal{R}_p . We are now going to argue that this obvious solution is in fact the only solution which is compatible with the positivity of the coefficients r_p . Let us factor out of $G(x)$ the exponential behavior it may contain by writing

$$G(x) = g(x) e^{\alpha x} , \quad (133)$$

where $g(x)$ is a function whose growth at infinity is bounded by a polynomial. The functional equation (132), when rewritten in terms of $g(x)$, implies

$$\forall x , \quad g(x+1) = g(x)g(1) , \quad (134)$$

and in particular

$$\forall n \in \mathbb{Z} , \quad g(n) = g(0)g^n(1) . \quad (135)$$

Since $g(x)$ cannot grow faster than a polynomial at infinity, we must therefore have $g(1) = 1$, and eq. (134) becomes

$$\forall x , \quad g(x+1) = g(x) . \quad (136)$$

Hence the function $g(x)$ must be a periodic function of period unity. This is where the positivity of the r_p 's plays a role: it implies that all the successive derivatives of $G(x)$ are positive for $x > 0$. In terms of $g(x)$, the n -th derivative of $G(x)$ reads

$$G^{(n)}(x) = e^{\alpha x} \sum_{p=0}^n C_n^p \alpha^{n-p} g^{(p)}(x) , \quad (137)$$

where the $C_n^p \equiv n!/p!(n-p)!$ are the binomial coefficients. We must therefore find a periodic function $g(x)$ such that

$$\forall n \in \mathbb{N} , \quad \forall x , \quad \sum_{p=0}^n C_n^p \alpha^{n-p} g^{(p)}(x) > 0 .. \quad (138)$$

Let us write the periodic function $g(x)$ as a Fourier series,

$$g(x) \equiv \sum_{l \in \mathbb{Z}} g_l e^{2i\pi l x} , \quad (139)$$

where $g_{-l} = g_l^*$ since $g(x)$ is real when x is real. The left hand side in the inequality (137) can be written as

$$g_0 \alpha^n + 2 \sum_{l=1}^{+\infty} |g_l| (\alpha^2 + 4\pi^2 l^2)^{n/2} \cos(2\pi l x + n\phi_l) , \quad (140)$$

where we parameterize $g_l(\alpha + 2i\pi l) \equiv |g_l| \sqrt{\alpha^2 + 4\pi^2 l^2} \exp(i\phi_l)$. We see that for any n and l , we can choose a value of x such that the cosine equals -1 . Moreover,

by going to sufficiently large n , we can make $(\alpha^2 + 4\pi^2 l^2)^{n/2}$ arbitrarily large compared to α^n . Therefore, the values of $|g_l|$ such that eq. (140) is always positive have to be chosen arbitrarily small. Therefore, we have proved that the only choice of the Fourier coefficients which is compatible with the positivity of the probabilities \mathcal{R}_p is

$$\forall l \in \mathbb{Z}^* , \quad g_l = 0 . \quad (141)$$

Thus, the function $g(x)$ is constant and equal to 1 (from $g(1) = 1$), and the only functions $G(x)$ that obey the functional relation (132) are the exponentials $G(x) = \exp(\alpha x)$. We have therefore proved that the only distributions \mathcal{R}_p that lead to the AGK cancellations are Poisson distributions.

D Discussion of the cancellations in eq. (109)

We will here study the cancellations in eq. (109) more explicitly. Note first that the terms in $g^{-2} \sum_r r b_r$ must correspond to the terms in the r.h.s. of eq. (109) topology by topology. For the simplest topology that appears in b_1/g^2 , only 1-particle cuts are allowed, and it is trivial to check the identity of eq. (109). The first non-trivial topology is the “star” diagram that appears in b_1/g^2 and in b_2/g^2 . Its contribution to the left hand side of eq. (109) is

$$\begin{aligned} \frac{1}{g^2} \sum_r r b_r |_{LO} = & \frac{1}{6} \text{---} \text{---} \text{---} + \frac{1}{6} \text{---} \text{---} \text{---} + \frac{1}{6} \text{---} \text{---} \text{---} + \frac{1}{6} \text{---} \text{---} \text{---} + \frac{1}{6} \text{---} \text{---} \text{---} + \frac{1}{6} \text{---} \text{---} \text{---} \\ & + \frac{1}{3} \text{---} \text{---} \text{---} + \frac{1}{3} \text{---} \text{---} \text{---} + \frac{1}{3} \text{---} \text{---} \text{---} + \frac{1}{3} \text{---} \text{---} \text{---} + \frac{1}{3} \text{---} \text{---} \text{---} + \frac{1}{3} \text{---} \text{---} \text{---} \end{aligned} \quad (142)$$

On the other hand, the contribution of this topology to the right hand side of eq. (109) is comprised of the terms

$$\frac{1}{2} \text{---} \text{---} \text{---} + \frac{1}{2} \text{---} \text{---} \text{---} + \frac{1}{2} \text{---} \text{---} \text{---} + \frac{1}{2} \text{---} \text{---} \text{---} + \frac{1}{2} \text{---} \text{---} \text{---} + \frac{1}{2} \text{---} \text{---} \text{---} \quad (143)$$

Note that we have discarded two vanishing terms, in which a vertex of type + (resp. -) was completely surrounded by sources of type - (resp. +), because such a configuration is forbidden by energy configuration (because of the $\theta(\pm p_0)$ factors in the Fourier transform of the propagators G_{-+} and G_{+-}). At this point, it is a trivial matter of inspection to check that eqs. (142) and (143) are identical. One should stress that it was crucial to weight the various r -particle cuts b_r/g^2 by the multiplicity r on the cut.

One can also see that the equivalence stated in eq. (109) between the method of calculating $\langle n \rangle$ from the classical field ϕ_c and the direct method implies that $b_2 \neq 0$ (in other words, this equivalence fails if one disregards the 2-particle cuts in eq. (142)). Incidentally, this proves that the distribution of produced particles is not a Poisson distribution, according to the discussion at the end of section 3.

References

- [1] I. Balitsky, L.N. Lipatov, Sov. J. Nucl. Phys. **28**, 822 (1978).
- [2] E.A. Kuraev, L.N. Lipatov, V.S. Fadin, Sov. Phys. JETP **45**, 199 (1977).
- [3] L.V. Gribov, E.M. Levin, M.G. Ryskin, Phys. Rept. **100**, 1 (1983).
- [4] A.H. Mueller, J-W. Qiu, Nucl. Phys. **B 268**, 427 (1986).
- [5] J.P. Blaizot, A.H. Mueller, Nucl. Phys. **B 289**, 847 (1987).
- [6] A.H. Mueller, Lectures given at the International Summer School on Particle Production Spanning MeV and TeV Energies (Nijmegen 99), Nijmegen, Netherlands, 8-20, Aug 1999, hep-ph/9911289.
- [7] L.D. McLerran, R. Venugopalan, Phys. Rev. **D 49**, 2233 (1994).
- [8] L.D. McLerran, R. Venugopalan, Phys. Rev. **D 49**, 3352 (1994).
- [9] L.D. McLerran, R. Venugopalan, Phys. Rev. **D 50**, 2225 (1994).
- [10] Yu.V. Kovchegov, Phys. Rev. **D 54**, 5463 (1996).
- [11] S. Jeon, R. Venugopalan, Phys. Rev. **D 70**, 105012 (2004).
- [12] S. Jeon, R. Venugopalan, Phys. Rev. **D 71**, 125003 (2005).
- [13] J. Jalilian-Marian, A. Kovner, L.D. McLerran, H. Weigert, Phys. Rev. **D 55**, 5414 (1997).
- [14] J. Jalilian-Marian, A. Kovner, A. Leonidov, H. Weigert, Nucl. Phys. **B 504**, 415 (1997).
- [15] J. Jalilian-Marian, A. Kovner, A. Leonidov, H. Weigert, Phys. Rev. **D 59**, 014014 (1999).
- [16] J. Jalilian-Marian, A. Kovner, A. Leonidov, H. Weigert, Phys. Rev. **D 59**, 034007 (1999).
- [17] J. Jalilian-Marian, A. Kovner, A. Leonidov, H. Weigert, Erratum. Phys. Rev. **D 59**, 099903 (1999).
- [18] E. Iancu, A. Leonidov, L.D. McLerran, Nucl. Phys. **A 692**, 583 (2001).
- [19] E. Iancu, A. Leonidov, L.D. McLerran, Phys. Lett. **B 510**, 133 (2001).
- [20] E. Ferreira, E. Iancu, A. Leonidov, L.D. McLerran, Nucl. Phys. **A 703**, 489 (2002).
- [21] I. Balitsky, Nucl. Phys. **B 463**, 99 (1996).
- [22] Yu.V. Kovchegov, Phys. Rev. **D 61**, 074018 (2000).

- [23] L.D. McLerran, Lectures given at the 40'th Schladming Winter School: Dense Matter, March 3-10 2001, hep-ph/0104285.
- [24] E. Iancu, A. Leonidov, L.D. McLerran, Lectures given at Cargese Summer School on QCD Perspectives on Hot and Dense Matter, Cargese, France, 6-18 Aug 2001, hep-ph/0202270.
- [25] E. Iancu, R. Venugopalan, Quark Gluon Plasma 3, Eds. R.C. Hwa and X.N.Wang, World Scientific, hep-ph/0303204.
- [26] A. Kovner, L.D. McLerran, H. Weigert, Phys. Rev. **D 52**, 3809 (1995).
- [27] A. Kovner, L.D. McLerran, H. Weigert, Phys. Rev. **D 52**, 6231 (1995).
- [28] Yu.V. Kovchegov, D.H. Rischke, Phys. Rev. **C 56**, 1084 (1997).
- [29] A. Krasnitz, R. Venugopalan, Nucl. Phys. **B 557**, 237 (1999).
- [30] A. Krasnitz, R. Venugopalan, Phys. Rev. Lett. **84**, 4309 (2000).
- [31] A. Krasnitz, R. Venugopalan, Phys. Rev. Lett. **86**, 1717 (2001).
- [32] A. Krasnitz, Y. Nara, R. Venugopalan, Nucl. Phys. **A 727**, 427 (2003).
- [33] A. Krasnitz, Y. Nara, R. Venugopalan, Phys. Rev. Lett. **87**, 192302 (2001).
- [34] T. Lappi, Phys. Rev. **C 67**, 054903 (2003).
- [35] P. Romatschke, R. Venugopalan, hep-ph/0510121, to appear in Phys. Rev. Lett.
- [36] F. Gelis, K. Kajantie, T. Lappi, Phys. Rev. C. **71**, 024904 (2005).
- [37] F. Gelis, K. Kajantie, T. Lappi, hep-ph/0508229, to appear in Phys. Rev. Lett.
- [38] R.E. Cutkosky, J. Math. Phys. **1**, 429 (1960).
- [39] V.A. Abramovsky, V.N. Gribov, O.V. Kancheli, Sov. J. Nucl. Phys. **18**, 308 (1974).
- [40] J.H. Weis, Acta Phys. Polon. **B 7**, 851 (1976).
- [41] J. Koplik, A.H. Mueller, Phys. Rev. **D 12**, 3638 (1975).
- [42] J. Bartels, M.G. Ryskin, Z. Phys. **C 76**, 241 (1997).
- [43] J. Bartels, M. Salvadore, G.P. Vacca, Eur. Phys. J. **C 42**, 53 (2005).
- [44] A.H. Mueller, Nucl. Phys. **B 415**, 373 (1994).
- [45] Yu.V. Kovchegov, E. Levin, Nucl. Phys. **B 577**, 221 (2000).
- [46] Yu.V. Kovchegov, K. Tuchin, Phys. Rev. **D 65**, 074026 (2002).

- [47] J. Jalilian-Marian, Y. Kovchegov, *Prog. Part. Nucl. Phys.* **56**, 104 (2006).
- [48] C. Itzykson, J.B. Zuber, *Quantum field theory*, McGraw-Hill (1980).
- [49] M.E. Peskin, D.V. Schroeder, *An introduction to quantum field theory*, Addison-Wesley, New-York (1995).
- [50] J. Schwinger, *J. Math. Phys.* **2**, 407 (1961).
- [51] L.V. Keldysh, *Sov. Phys. JETP* **20**, 1018 (1964).
- [52] G. 'tHooft, M.J.G. Veltman, CERN report 73-9.
- [53] M.J.G. Veltman, *Physica* **29**, 186 (1963).
- [54] D. Vaman, Y.P. Yao, hep-th/0512031.
- [55] A.J. Baltz, F. Gelis, L.D. McLerran, A. Peshier, *Nucl. Phys.* **A 695**, 395 (2001).
- [56] P. Aurenche, T. Becherrowy, *Nucl. Phys.* **B 379**, 259 (1992).
- [57] M.A. van Eijck, R. Kobes, Ch.G. van Weert, *Phys. Rev.* **D 50**, 4097 (1994).
- [58] J.P. Blaizot, F. Gelis, R. Venugopalan, *Nucl. Phys.* **A 743**, 57 (2004).
- [59] J.P. Blaizot, F. Gelis, R. Venugopalan, *Nucl. Phys.* **A 743**, 13 (2004).
- [60] D. Dietrich, hep-th/0512026.
- [61] M. Gyulassy, I. Vitev, X.N. Wang, B.N. Zhang, *Quark Gluon Plasma 3*, editors: R.C. Hwa and X.N. Wang, World Scientific, Singapore, nucl-th/0302077.
- [62] R. Baier, D. Schiff, B.G. Zakharov, *Ann. Rev. Nucl. Part. Sci.* **50**, 37 (2000).
- [63] A. Kovner, U. Wiedemann, hep-ph/0304151.
- [64] R. Baier, A.H. Mueller, D. Schiff, D. Son, *Phys. Lett.* **B 502**, 51 (2001).
- [65] A.H. Mueller, A.I. Shoshi, S.M.H. Wong, *Phys. Lett.* **B 632**, 257 (2006).
- [66] P. Arnold, J. Lenaghan, G.D. Moore, L.G. Yaffe, *Phys. Rev. Lett.* **94**, 072302 (2005).
- [67] A.K. Rebhan, P. Romatschke, M. Strickland, *Phys. Rev. Lett.* **94**, 102303 (2005).
- [68] S. Mrowczynski, hep-ph/0511052.
- [69] D. Kharzeev, K. Tuchin, *Nucl. Phys.* **A 753**, 316 (2005).
- [70] F. Gelis, S. Jeon, R. Venugopalan, work in progress.

- [71] A.H. Mueller, D.T. Son, Phys. Lett. **B 582**, 279 (2004).
- [72] S. Jeon, Phys. Rev. **C 72**, 014907 (2005).
- [73] M. Le Bellac, *Thermal field theory*, Cambridge University Press (1996).